Computer Modeling in Engineering & Sciences

Tech Science Press

DOI: 10.32604/cmes.2023.028826

ARTICLE

Reliability Analysis of HEE Parameters via Progressive Type-II Censoring with Applications

Heba S. Mohammed[1], Mazen Nassar[2,3], Refah Alotaibi[1] and Ahmed Elshahhat[4,*]

[1]Department of Mathematical Sciences, College of Science, Princess Nourah bint Abdulrahman University, P.O. Box 84428, Riyadh, 11671, Saudi Arabia

[2]Department of Statistics, Faculty of Science, King Abdulaziz University, Jeddah, 21589, Saudi Arabia

[3]Department of Statistics, Faculty of Commerce, Zagazig University, Zagazig, Egypt

[4]Faculty of Technology and Development, Zagazig University, Zagazig, 44519, Egypt

*Corresponding Author: Ahmed Elshahhat. Email: aelshahhat@ftd.zu.edu.eg

Received: 10 January 2023 Accepted: 21 March 2023 Published: 03 August 2023

ABSTRACT

A new extended exponential lifetime model called Harris extended-exponential (HEE) distribution for data modelling with increasing and decreasing hazard rate shapes has been considered. In the reliability context, researchers prefer to use censoring plans to collect data in order to achieve a compromise between total test time and/or test sample size. So, this study considers both maximum likelihood and Bayesian estimates of the Harris extended-exponential distribution parameters and some of its reliability indices using a progressive Type-II censoring strategy. Under the premise of independent gamma priors, the Bayesian estimation is created using the squared-error and general entropy loss functions. Due to the challenging form of the joint posterior distribution, to evaluate the Bayes estimates, samples from the full conditional distributions are generated using Markov Chain Monte Carlo techniques. For each unknown parameter, the highest posterior density credible intervals and asymptotic confidence intervals are also determined. Through a simulated study, the usefulness of the various suggested strategies is assessed. The optimal progressive censoring plans are also shown, and various optimality criteria are investigated. Two actual data sets, taken from engineering and veterinary medicine areas, are analyzed to show how the offered point and interval estimators can be used in practice and to verify that the proposed model furnishes a good fit than other lifetime models: alpha power exponential, generalized-exponential, Nadarajah-Haghighi, Weibull, Lomax, gamma and exponential distributions. Numerical evaluations revealed that in the presence of progressively Type-II censored data, the Bayes estimation method against the squared-error (symmetric) loss is advised for getting the point and interval estimates of the HEE distribution.

KEYWORDS

Harris extended-exponential model; progressive Type-II censoring; reliability; maximum likelihood; MCMC techniques; Monte Carlo experiments

1 Introduction

Modelling actual data using generalized distributions is still important today. A variety of generalized distributions have been developed, and their usefulness in various contexts is investigated, see for example the work of Nadarajah et al. [1] and Mahdavi et al. [2]. By combining the exponential and Harris distributions, Pinho et al. [3] created a new three-parameter lifetime model known as the Harris extended-exponential (HEE) distribution. They emphasized that the HEE distribution can be utilized as a substitute of the Weibull and gamma distributions for modelling data with a rising or decreasing failure rate. As a result, it can be applied in a variety of domains, including but not limited to reliability, biology, engineering, insurance and epidemiology, among others.

However, if X is a random variable that follows the HEE distribution, denoted by $X \sim \text{HEE}(\boldsymbol{\Psi})$, where $\boldsymbol{\Psi} = (\alpha, \beta, \theta)^\top$ is the parameters vector with scale parameter β and shape parameters α and θ, then its probability density function (PDF) and cumulative distribution function (CDF) can be written, respectively, as

$$f(x;\boldsymbol{\Psi}) = \frac{\beta\theta^{\frac{1}{\alpha}} e^{-\beta x}}{[1-\bar{\theta}e^{-\alpha\beta x}]^{1+\frac{1}{\alpha}}}, \quad x > 0, \quad \alpha, \beta, \theta > 0, \tag{1}$$

and

$$F(x;\boldsymbol{\Psi}) = 1 - \left[\frac{\theta e^{-\alpha\beta x}}{1-\bar{\theta}e^{-\alpha\beta x}}\right]^{\frac{1}{\alpha}}, \tag{2}$$

where $\bar{\theta} = 1 - \theta$. One can see that when $\alpha = 1$, the HEE distribution reduces to the Marshall–Olkin exponential distribution proposed by Marshall et al. [4]. Also, the exponential distribution can be obtained as a special case from the HEE distribution by putting $\alpha = \theta = 1$. The associated reliability characteristics of X such as reliability function (RF) and hazard rate function (HRF), at mission time t, are expressed, respectively, as follows:

$$R(t;\boldsymbol{\Psi}) = \left[\frac{\theta e^{-\alpha\beta t}}{1-\bar{\theta}e^{-\alpha\beta t}}\right]^{\frac{1}{\alpha}} \tag{3}$$

and

$$h(t;\boldsymbol{\Psi}) = \beta[1-\bar{\theta}e^{-\alpha\beta t}]^{-1}. \tag{4}$$

Fig. 1a displays different plots of the PDF using various choices of parameters. Similarly, Fig. 1b shows the plots of the HRF. Fig. 1a indicates that the PDF of the HEE distribution can be decreasing or unimodal. On the other hand, its HRF allows for decreasing and increasing shape hazard rates.

In reliability analysis and life testing studies, the examined items are commonly lost or discarded before failure. The obtained sample is therefore known as a censored sample. To preserve the functional experimental units for future use, shortening the duration of the test, and saving money are some major justifications for removing the experimental units. Various censoring techniques, such as time and failure censoring, are available in the literature; nevertheless, they do not have the ability to permit units to be eliminated at any moment other than the experiment's endpoint. As a result, a more flexible censoring scheme known as progressive Type-II censoring is offered. For more in-depth analysis, or to be used as test samples in other research, certain items may need to be removed from the experiment.

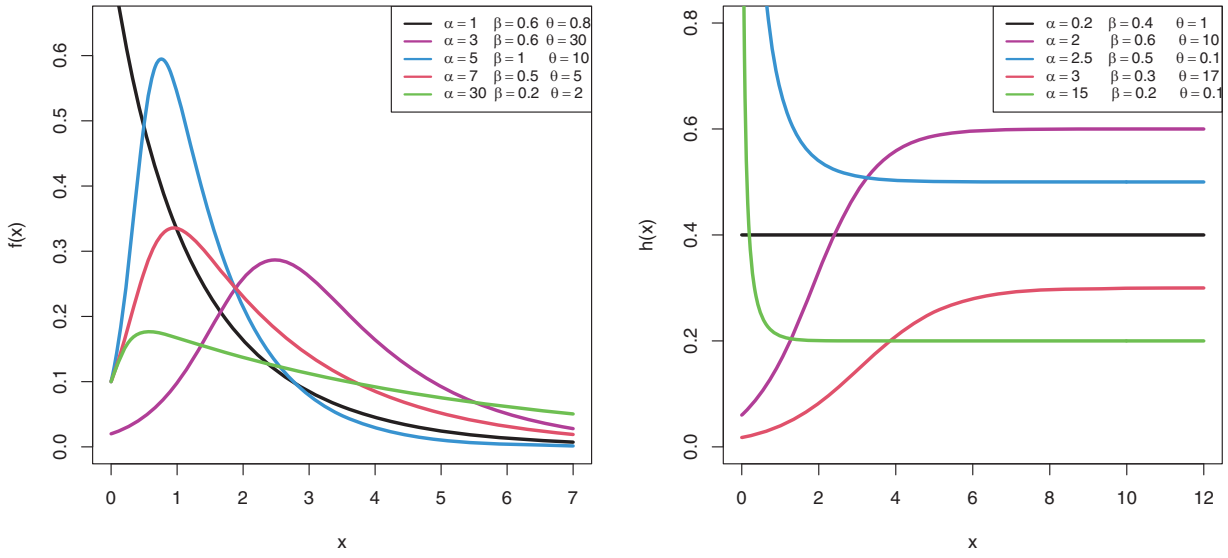

(a) PDF (b) HRF

Figure 1: Shapes of the PDF and HRF of the HEE distribution

The schematic representation of the progressive Type-II censoring scheme is as follows: Assume that m units will fail out of n distinct units that are put on a life test. Allow $(R_1, R_2, \ldots, R_m)$ to be fixed in advance such that when the first failure occurs, $X_{1:m:n}$, R_1 units are arbitrarily removed from the experiment. When the experiment has its second failure, $X_{2:m:n}$, R_2 units from the remaining items are at random deleted from the test, and so on. When the m^{th} failure $X_{m:m:n}$ occurred, all R_m remaining items are extracted from the test. It is clear that $n = m + \sum_{i=1}^{m} R_i$. When $R_i = 0, i = 1, \ldots, m-1$ and $R_m = n - m$, the case of conventional Type-II censored sampling arises. The progressive Type II censoring plan reduces to the case of a complete sample when $R_i = 0, i = 1, \ldots, m$. If we assume that a continuous population with CDF $F(\cdot)$, and PDF $f(\cdot)$, then the likelihood function for a progressively Type-II censored sample can be expressed as below:

$$L(\boldsymbol{\Psi}) = C \prod_{i=1}^{m} f(x_{i:m:n})[1 - F(x_{i:m:n})]^{R_i}, \tag{5}$$

where $C = n(n - R_1 - 1)\ldots(n - \sum_{i=1}^{m-1}(1 + R_i))$. Many studies used progressively Type-II censored data to consider some estimation issues for various lifetime distributions.

In literature, different censoring schemes were introduced; however, authors prefer to deal with progressive censoring over other censoring plans because it allows survival items to be withdrawn during the experiment at different stages which is not possible in case of failure (Type-II) censoring. Sultan et al. [5] investigated the classical and Bayesian estimation of inverse Weibull distribution. Dey et al. [6] investigated the maximum likelihood and Bayesian estimations for Marshall–Olkin extended exponential distribution. Kotb et al. [7] studied the inferences for modified Weibull distribution. Bdair et al. [8] analyzed the estimation and prediction for flexible Weibull distribution. Wu et al. [9] discussed the estimation and prediction problems for the Nadarajah–Haghighi parameters. Alotaibi et al. [10] considered the estimation of some reliability indices for alpha power Weibull

distribution. Elshahhat et al. [11] considered the Bayesian life analysis of generalized Chen's parameters. Dey et al. [12] studied various inferences for the Wilson–Hilferty parameters. For additional details regarding the concept of progressive censoring, one can guide Balakrishnan et al. [13].

Despite the flexibility and adaptability of the HEE distribution in modelling different types of data, to the best of our knowledge, there is no existing study on censoring mechanisms that deals with the estimation of parameters and/or reliability characteristics of the HEE distribution under incomplete (censored) sampling, which is of great interest and practical importance in many real-world scenarios. So, this study stands out in that it is the first to investigate the estimation issues for the HEE distribution when using incomplete data collected from a progressively Type-II censoring. Consequently, the main purposes for this study are fourfold:

- First objective explores various point and interval estimation issues of the HEE distribution parameters as well as its reliability characteristics utilizing progressive Type-II censored data, namely: maximum likelihood estimators (MLEs), Bayes estimators, approximate confidence intervals (ACIs) and highest posterior density (HPD) credible intervals.
- In Bayesian analysis, utilizing Markov Chain Monte Carlo (MCMC) techniques, the estimators are acquired by employing the squared-error (SE) and general entropy (GE) loss functions.
- The second objective performs extensive Monte Carlo simulations to compare the performance of the proposed estimation methods on the basis of their simulated root mean squared errors, mean absolute biases, average confidence lengths and coverage probabilities.
- The third objective is to check various optimality criteria to decide the best progressive censoring schemes.
- The last one is to demonstrate the ability of the proposed methods to work in practice by exploring two actual real data sets.

Before going any further, it is important to remember that the limitations of this study are: (i) All inferential methodologies are developed based on the assumption that at least one survival item was removed during the life-test; (ii) We assumed that the HEE parameters α, β and θ as well as its related parametric functions $R(t)$ and $h(t)$ are unknown.

The remaining sections of the study are organized as follows: Section 2 presents MLEs and ACIs. Section 3 investigates the Bayes estimators and HPD credible intervals. The results of the simulation study are included in Section 4. We offer several ways to select the optimum censoring scheme in Section 5. Section 6 highlights the analysis of two real data applications. The paper is finally concluded in Section 7.

2 Likelihood Inference

In this section, the MLEs of the unknown parameters including the RF and HRF of the HEE distribution are investigated. Moreover, the ACIs based on the asymptotic properties of the MLEs are constructed. Assume that $\underline{x} = (x_1, \ldots, x_m)$, where $x_i = x_{i:m:n}, i = 1, \ldots, m$, for simplicity, be a progressively Type-II censored sample selected from a population with PDF and CDF given by (1) and (2), respectively. Given a predetermined progressive censoring scheme $R_1, \ldots, R_m$, then the likelihood function, without the constant term, can be derived from (1), (2) and (5) as follows:

$$L(\boldsymbol{\Psi}|\underline{x}) = \beta^m \theta^{\frac{n}{\alpha}} e^{-\beta \sum_{i=1}^{m} R_i^* x_i} \prod_{i=1}^{m} \left[1 - \bar{\theta} e^{-\alpha \beta x_i}\right]^{-(1+\bar{\alpha} R_i^*)}, \tag{6}$$

where $R_i^* = 1 + R_i$ and $\bar{\alpha} = 1/\alpha$. Instead of maximizing the likelihood function in (6), it is more convenient to work with its natural logarithm. Thus, it follows:

$$\ell(\boldsymbol{\Psi}|\underline{x}) = m\log(\beta) + \frac{n}{\alpha}\log(\theta) - \beta\sum_{i=1}^{m} R_i^* x_i - \sum_{i=1}^{m}(1+\bar{\alpha}R_i^*)\log\left[1-\bar{\theta}e^{-\alpha\beta x_i}\right], \tag{7}$$

where $\ell(\boldsymbol{\Psi}|\underline{x}) = \log L(\boldsymbol{\Psi}|\underline{x})$. The MLEs of α, β and θ, denoted by $\hat{\alpha}, \hat{\beta}$ and $\hat{\theta}$, are obtained by maximizing (7) with respect to α, β and θ. An equivalent way to obtain the MLEs is to solve the three normal equations simultaneously, which are acquired by getting the first order derivatives of the objective function in (7) with respect to the unknown parameters and equating the result by zero. Consequently, the normal equations are

$$\frac{\partial\ell(\boldsymbol{\Psi}|\underline{x})}{\partial\alpha} = -\frac{n\log(\beta)}{\alpha^2} + \frac{1}{\alpha^2}\sum_{i=1}^{m} R_i^*\log\left[1-\bar{\theta}v_i\right] - \beta\bar{\theta}\sum_{i=1}^{m}(1+\bar{\alpha}R_i^*)\frac{x_i v_i}{1-\bar{\theta}v_i} = 0, \tag{8}$$

$$\frac{\partial\ell(\boldsymbol{\Psi}|\underline{x})}{\partial\beta} = \frac{m}{\beta} - \sum_{i=1}^{m} R_i^* x_i - \alpha\bar{\theta}\sum_{i=1}^{m}(1+\bar{\alpha}R_i^*)\frac{x_i v_i}{1-\bar{\theta}v_i} = 0 \tag{9}$$

and

$$\frac{\partial\ell(\boldsymbol{\Psi}|\underline{x})}{\partial\theta} = \frac{n}{\alpha\theta} - \sum_{i=1}^{m}(1+\bar{\alpha}R_i^*)\frac{v_i}{1-\bar{\theta}v_i} = 0, \tag{10}$$

where $v_i = e^{-\alpha\beta x_i}$. It is clear from (8)–(10), that the MLEs $\hat{\alpha}$, $\hat{\beta}$ and $\hat{\theta}$ have no closed forms. Therefore, numerical methods may be implemented to solve these equations to produce $\hat{\alpha}, \hat{\beta}$ and $\hat{\theta}$. Since the MLE of α, β or θ cannot be solved analytically, the 'maxLik' package (which implements the Newton–Raphson (NR) method of maximization) proposed by Henningsen et al. [14] can be easily used. On the other hand, instead of NR method, the expectation–maximization (EM) or stochastic EM algorithm can be easily incorporated. For details, see Panahi [15,16].

Once the MLEs of α, β and θ are obtained, we can get the MLEs of $R(t)$ and $h(t)$ by using the invariance property of the MLEs as follows:

$$\hat{R}(t) = \left[\frac{\hat{\theta}e^{-\hat{\alpha}\hat{\beta}t}}{1-\hat{\bar{\theta}}e^{-\hat{\alpha}\hat{\beta}t}}\right]^{\frac{1}{\hat{\alpha}}}, \quad \text{and} \quad \hat{h}(t) = \hat{\beta}[1-\hat{\bar{\theta}}e^{-\hat{\alpha}\hat{\beta}t}]^{-1},$$

where $\hat{\bar{\theta}} = 1 - \hat{\theta}$.

After getting the point estimates of α, β and θ as well as the reliability indices, it is also of appeal to construct the associated confidence intervals. This objective can be achieved by employing the asymptotic properties of the MLEs. It is known that based on the theory of large samples that the asymptotic distribution of $\hat{\boldsymbol{\Psi}}$, where $\hat{\boldsymbol{\Psi}} = (\hat{\alpha}, \hat{\beta}, \hat{\theta})^\top$, is normal distribution with average $\hat{\boldsymbol{\Psi}}$ and variance-covariance matrix $\boldsymbol{I}_{3\times3}^{-1}(\boldsymbol{\Psi})$ which is obtained by taking the inverse of the Fisher information (FI) matrix. It is not easy to obtain the elements of the FI matrix due to its intractable elements. Therefore, we can use the observed FI matrix to obtain $\boldsymbol{I}_{3\times3}^{-1}(\hat{\boldsymbol{\Psi}})$ as an estimate of $\boldsymbol{I}_{3\times3}^{-1}(\boldsymbol{\Psi})$, where

$$I_{3\times3}^{-1}(\hat{\boldsymbol{\Psi}}) = \begin{bmatrix} -F_{\alpha\alpha} & -F_{\alpha\beta} & -F_{\alpha\theta} \\ -F_{\beta\alpha} & -F_{\beta\beta} & -F_{\beta\theta} \\ -F_{\theta\alpha} & -F_{\theta\beta} & -F_{\theta\theta} \end{bmatrix}^{-1}_{(\alpha,\beta,\theta)=(\hat{\alpha},\hat{\beta},\hat{\theta})} = \begin{bmatrix} \hat{\sigma}_{\alpha\alpha} & \hat{\sigma}_{\alpha\beta} & \hat{\sigma}_{\alpha\theta} \\ & \hat{\sigma}_{\beta\beta} & \hat{\sigma}_{\beta\theta} \\ & & \hat{\sigma}_{\theta\theta} \end{bmatrix}, \tag{11}$$

where the main diagonal elements are the estimated variances of $\hat{\alpha}, \hat{\beta}$ and $\hat{\theta}$, respectively, and the elements of the observed FI matrix can be easily obtained from (7) as follows:

$$\frac{\partial^2 \ell(\boldsymbol{\Psi}|\underline{x})}{\partial \alpha^2} = \frac{2n\log(\theta)}{\alpha^2} - \frac{2}{\alpha^3}\sum_{i=1}^{m} R_i^* \log\left[1-\bar{\theta}v_i\right] + \beta\bar{\theta}\sum_{i=1}^{m}\frac{x_i v_i}{1-\bar{\theta}v_i}\left[\frac{2R_i^*}{\alpha^2} + \frac{\beta x_i(1+\bar{\alpha}R_i^*)}{1-\bar{\theta}v_i}\right],$$

$$\frac{\partial^2 \ell(\boldsymbol{\Psi}|\underline{x})}{\partial \beta^2} = -\frac{m}{\beta^2} + \bar{\theta}\alpha^2\sum_{i=1}^{m}(1+\bar{\alpha}R_i^*)\frac{v_i x_i^2}{(1-\bar{\theta}v_i)^2},$$

$$\frac{\partial^2 \ell(\boldsymbol{\Psi}|\underline{x})}{\partial \theta^2} = -\frac{n}{\alpha\theta^2} + \sum_{i=1}^{m}(1+\bar{\alpha}R_i^*)\frac{v_i^2}{(1-\bar{\theta}v_i)^2},$$

$$\frac{\partial^2 \ell(\boldsymbol{\Psi}|\underline{x})}{\partial \alpha\partial \beta} = -\bar{\theta}\sum_{i=1}^{m}\frac{x_i v_i}{1-\bar{\theta}v_i} + \bar{\theta}\alpha\beta\sum_{i=1}^{m}(1+\bar{\alpha}R_i^*)\frac{v_i x_i^2}{(1-\bar{\theta}v_i)^2},$$

$$\frac{\partial^2 \ell(\boldsymbol{\Psi}|\underline{x})}{\partial \alpha\partial \theta} = -\frac{n}{\alpha\theta^2} + \frac{1}{\alpha^2}\sum_{i=1}^{m} R_i^*\frac{v_i}{1-\bar{\theta}v_i} + \beta\sum_{i=1}^{m}(1+\bar{\alpha}R_i^*)\frac{x_i v_i}{1-\bar{\theta}v_i}\left[1+\frac{\bar{\theta}v_i}{1-\bar{\theta}v_i}\right]$$

and

$$\frac{\partial^2 \ell(\boldsymbol{\Psi}|\underline{x})}{\partial \beta\partial \theta} = \alpha\sum_{i=1}^{m}(1+\bar{\alpha}R_i^*)\frac{x_i v_i}{(1-\bar{\theta}v_i)^2}.$$

Now, the $100(1-\gamma)\%$ ACIs of α, β and θ can be acquired as follows:

$$\hat{\alpha} \pm z_{\gamma/2}\sqrt{\sigma_{\alpha\alpha}}, \quad \hat{\beta} \pm z_{\gamma/2}\sqrt{\sigma_{\beta\beta}} \quad \text{and} \quad \hat{\theta} \pm z_{\gamma/2}\sqrt{\sigma_{\theta\theta}},$$

where $z_{\gamma/2}$ is the upper $(\gamma/2)^{th}$ percentile point of the standard normal distribution.

On the other hand, the ACIs of the RF and HRF can be also obtained by approximating the variances of their estimators by using the delta method. See Greene [17] for more details about the delta method. In this case, we can approximate the variances of $\hat{R}(t)$ and $\hat{h}(t)$ by $\hat{\sigma}_R = D_R I_{3\times 3}^{-1}(\hat{\boldsymbol{\Psi}})D_R^{\top}$ and $\hat{\sigma}_h = D_h I_{3\times 3}^{-1}(\hat{\boldsymbol{\Psi}})D_h^{\top}$, respectively, where

$$D_R = \left(\frac{\partial R(t)}{\partial \alpha}, \frac{\partial R(t)}{\partial \beta}, \frac{\partial R(t)}{\partial \theta}\right)\Big|_{(\alpha,\beta,\theta)=(\hat{\alpha},\hat{\beta},\hat{\theta})}$$

and

$$D_h = \left(\frac{\partial h(t)}{\partial \alpha}, \frac{\partial h(t)}{\partial \beta}, \frac{\partial h(t)}{\partial \theta}\right)\Big|_{(\alpha,\beta,\theta)=(\hat{\alpha},\hat{\beta},\hat{\theta})},$$

with the following elements

$$\frac{\partial R(t)}{\partial \alpha} = -\frac{1}{\alpha^2}\left(\frac{\theta v_t}{1-\bar{\theta}v_t}\right)^{\frac{1}{\alpha}}\left[\log\left(\frac{\theta v_t}{1-\bar{\theta}v_t}\right) + \frac{\alpha\beta t}{1-\bar{\theta}v_t}\right],$$

$$\frac{\partial R(t)}{\partial \beta} = -(1-\bar{\theta}v_t)^{-1}\left(\frac{\theta v_t}{1-\bar{\theta}v_t}\right)^{\frac{1}{\alpha}}, \quad \frac{\partial R(t)}{\partial \theta} = \frac{v_t - 1}{\alpha\theta(1-\bar{\theta}v_t)}\left(\frac{\theta t^{\alpha} v_t}{1-\bar{\theta}v_t},\right)^{\frac{1}{\alpha}}$$

$$\frac{\partial h(t)}{\partial \alpha} = -\frac{t\bar{\theta}\beta^2 v_t}{(1-\bar{\theta}v_t)^2}, \quad \frac{\partial h(t)}{\partial \beta} = \frac{1-\bar{\theta}v_t(1+\beta\alpha t)}{(1-\bar{\theta}v_t)^2}, \text{ and } \frac{\partial h(t)}{\partial \theta} = -\frac{\beta v_t}{(1-\bar{\theta}v_t)^2},$$

where $v_t = e^{-\alpha\beta t}$. Based on the above results, the ACIs for RF and HRF at the confidence level $100(1-\gamma)\%$ can be expressed, respectively, as

$$\hat{R} \pm z_{\frac{\gamma}{2}}\sqrt{\hat{\sigma}_R} \quad \text{and} \quad \hat{h} \pm z_{\frac{\gamma}{2}}\sqrt{\hat{\sigma}_h}.$$

Though the main problem of ACI for a positive parameter is that it may give a negative value in the lower bound. In literature, there are different approaches available to handle this problem. Theoretically, one of them is called the log-transformed maximum likelihood estimator developed by Meeker et al. [18]. Numerically, one can easily verify that the computed confidence intervals contain a lower bound with a positive value if one of them contains a negative lower bound, in which case this value is replaced by zero. Recently, this issue has been examined by Elshahhat et al. [11] and Elshahhat et al. [19].

3 Bayes MCMC Inference

In this section, we consider the Bayesian estimation method to derive the Bayesian estimators for α, β and θ, as well as the $R(t)$ and $h(t)$. Besides the point estimates, we also acquire the HPD credible intervals for the different parameters. In statistical analysis, the Bayesian method has significant advantages over the classical methods when data availability is a critical barrier. In Bayesian inference, prior distribution selection is important. Since the gamma density prior, based on its parameter values, provides various shapes, see Dey et al. [20]. Thus, it is flexible and can be adopted as a suitable prior for the HEE parameters. Therefore, we utilize the Bayesian estimation under the assumption that the unknown model parameters α, β and θ are independent and follow gamma (G) distributions, i.e., $\alpha \sim G(a_1, b_1)$, $\beta \sim G(a_2, b_2)$ and $\theta \sim G(a_3, b_3)$, where a_k and $b_k, k = 1, 2, 3$, are the hyper-parameters and are always positive. Using these premises, we can simply write the joint prior distribution of α, β and θ in the following form:

$$g(\boldsymbol{\Psi}) \propto \alpha^{a_1-1}\,\beta^{a_2-1}\,\theta^{a_3-1}\,e^{-(b_1\alpha+b_2\beta+b_3\theta)}. \tag{12}$$

To get the Bayes estimates, we should first derive the joint posterior distribution of the unknown parameters. To obtain the joint posterior distribution, we combine the sample information given by (6) with the prior information about the unknown parameters given by (12) and apply the Bayes theorem. As a result, we can write the joint posterior distribution as follows:

$$\pi(\boldsymbol{\Psi}|\underline{x}) = A^{-1}\alpha^{a_1-1}\beta^{m+a_2-1}\theta^{\frac{n}{\alpha}+a_3-1}e^{-\beta\left(\sum_{i=1}^{m} R_i^* x_i+b_2\right)-(b_1\alpha+b_3\theta)}\prod_{i=1}^{m}\left[1-\bar{\theta}e^{-\alpha\beta x_i}\right]^{-(1+\tilde{\alpha}R_i^*)}, \tag{13}$$

where A is the normalized constant and obtained as

$$A = \int_0^\infty\int_0^\infty\int_0^\infty \alpha^{a_1-1}\beta^{m+a_2-1}\theta^{\frac{n}{\alpha}+a_3-1}e^{-\beta\left(\sum_{i=1}^{m} R_i^* x_i+b_2\right)-(b_1\alpha+b_3\theta)}\prod_{i=1}^{m}\left[1-\bar{\theta}e^{-\alpha\beta x_i}\right]^{-(1+\tilde{\alpha}R_i^*)} d\alpha\, d\beta\, d\theta.$$

The loss function is crucial to Bayesian analysis because it may be used to characterize over-estimation and underestimation in the investigation. Symmetric and asymmetric loss are two often employed loss functions. While the asymmetric loss function offers various weights to overestimation and underestimation, the symmetric loss function treats overestimation and underestimation equally. The asymmetric loss is more practical and advantageous in real-world applications than the symmetric loss see for more details Nassar et al. [21]. One of the most popular symmetric loss functions is the SE loss function, whereas the GE loss function is asymmetric. The SE and GE loss functions are considered in this work to acquire the Bayes estimates. It is generally known that the posterior mean

is the Bayes estimator in the case of the SE loss function. On the other hand, the GE loss function provides varying weights for overestimation and underestimation.

Let $\tilde{\mu}$ is an estimator of μ, then according to Calabria et al. [22], the GE loss function can be expressed as

$$E(\tilde{\mu},\mu) \propto (\tilde{\mu}/\mu)^{\delta} - \delta \log(\mu/\mu) - 1, \quad \delta \neq 0,$$

where δ determines the degree of asymmetry. In this case, the Bayes estimator of δ can be obtained as

$$\tilde{\mu}_{GE} = \left[E_{\mu}(\mu^{-\delta})\right]^{-\frac{1}{\delta}}, \tag{14}$$

given that $E_{\mu}(\mu^{-\delta})$ exists and is finite. Assume that $\Phi(\boldsymbol{\Psi})$ be any function of the unknown parameters. Therefore, the Bayes estimators of $\Phi(\boldsymbol{\Psi})$ based on SE and GE loss functions can be obtained, respectively, as

$$\tilde{\Phi}_{SE}(\boldsymbol{\Psi}) = \int_0^{\infty}\int_0^{\infty}\int_0^{\infty} \Phi(\boldsymbol{\Psi})\,\pi(\boldsymbol{\Psi}|\underline{x})\,d\alpha\,d\beta\,d\theta \tag{15}$$

and

$$\tilde{\Phi}_{GE}(\boldsymbol{\Psi}) = \left[\int_0^{\infty}\int_0^{\infty}\int_0^{\infty} [\Phi(\boldsymbol{\Psi})]^{-\delta}\,\pi(\boldsymbol{\Psi}|\underline{x})\,d\alpha\,d\beta\,d\theta\right]^{-\frac{1}{\delta}}, \tag{16}$$

where $\pi(\boldsymbol{\Psi}|\underline{x})$ is the joint posterior distribution given by (13). It is obvious that it is impossible to calculate the Bayes estimators using (15) and (16) analytically due to the complex forms of the integration. In order to acquire the Bayes estimates of the unknown parameters and the corresponding HPD credible intervals in this case, we suggest using the MCMC technique. We first must establish the full conditional distributions of α, β and θ before we can use the MCMC approach. Given (13), the necessary full conditional distributions can be determined as below:

$$\pi(\alpha|\beta,\theta,\underline{x}) \propto \alpha^{a_1-1}\theta^{\frac{n}{\alpha}}e^{-b_1\alpha}\prod_{i=1}^{m}\left[1-\bar{\theta}e^{-\alpha\beta x_i}\right]^{-(1+\bar{\alpha}R_i^*)}, \tag{17}$$

$$\pi(\beta|\alpha,\theta,\underline{x}) \propto \beta^{m+a_2-1}e^{-\beta\left(\sum_{i=1}^{m}R_i^*x_i+b_2\right)}\prod_{i=1}^{m}\left[1-\bar{\theta}e^{-\alpha\beta x_i}\right]^{-(1+\bar{\alpha}R_i^*)} \tag{18}$$

and

$$\pi(\theta|\alpha,\beta,\underline{x}) \propto \theta^{\frac{n}{\alpha}+a_3-1}e^{-b_3\theta}\prod_{i=1}^{m}\left[1-\bar{\theta}e^{-\alpha\beta x_i}\right]^{-(1+\bar{\alpha}R_i^*)}. \tag{19}$$

Even though we have the full conditional distributions for each parameter, they do not have a known form, making it difficult to directly take samples from them. Therefore, we utilize the Metropolis–Hasting (M–H) algorithm to generate samples from these distributions. In order to derive the Bayesian estimates and the HPD credible intervals, we assume the normal distribution as the proposal distribution for the M–H sampling. Using the full conditional distributions given by (17)–(19), the required steps for the MH algorithm are as below

Step 1. Start with $p = 1$.

Step 2. Determine the beginning values such that $\left(\alpha^{(0)},\beta^{(0)},\theta^{(0)}\right) = (\hat{\alpha},\hat{\beta},\hat{\theta})$.

Step 3. Generate $\alpha^{(p)}$ from (17) using the M-H steps and $N\left(\alpha^{(p-1)}, \hat{\sigma}_{\alpha\alpha}\right)$.

Step 4. From (18) and (19), generate $\beta^{(p)}$ and $\theta^{(p)}$, respectively, by repeating Step 3.

Step 5. Use the generated sample $\left(\alpha^{(p)}, \beta^{(p)}, \theta^{(p)}\right)$ to obtain $R^{(p)}(t)$ and $h^{(p)}(t)$ from (3) and (4), respectively.

Step 6. Put $p = p + 1$.

Step 7. Replicate Steps 3–6, N times to get $\alpha^{(p)}, \beta^{(p)}, \theta^{(p)}, R^{(p)}(t)$ and $h^{(p)}(t), p = 1, \ldots, N$.

In order to ensure convergence and remove the appeal of initial values, the first B generated variates are discarded. In this instance, we possess $\alpha^{(p)}, \beta^{(p)}, \theta^{(p)}, R^{(p)}(t)$ and $h^{(p)}(t)$, where $p = B + 1, \ldots, N$. The resulting sample, which is based founded on a big B, delivers an approximately posterior sample that can be applied to compute the Bayes estimates as well as the HPD credible intervals.

Let ϕ denote the parameter that needs to be estimated. Following that, the SE loss function-based Bayes estimate of ϕ can be calculated as

$$\tilde{\phi}_{SE} = \frac{1}{N-B} \sum_{p=B+1}^{N} \phi^{(p)}.$$

Likewise, the following formula can be applied to obtain the Bayes estimate of ϕ based on the GE loss function.

$$\tilde{\phi}_{GE} = \left\{ \frac{1}{N-B} \sum_{p=B+1}^{N} [\phi^{(p)}]^{-\delta} \right\}^{-\frac{1}{\delta}}.$$

The HPD credible interval specifies a range that covers the majority of the distribution, say $100(1-\gamma)\%$ of it, and each point within the range has higher credibility than any point outside the range. To obtain the HPD credible intervals of $\alpha, \beta, \theta, R(t)$ and $h(t)$, say ϕ, we order $\phi^{(p)}$, as $\phi^{(B+1)} < \phi^{(B+2)} < \cdots < \phi^{(N)}$. Then, the $100(1-\gamma)\%$ HPD credible interval of ϕ is $\left[\phi^{(p^*)}, \phi^{(p^*+(1-\gamma)(N-B))}\right]$, where $p^* = B+1, B+2, \ldots, N$ is defined in a way that

$$\phi^{(p^*+[(1-\gamma)(N-B)])} - \phi^{(p^*)} = \min_{1 \leqslant p \leqslant \gamma(N-B)} \left[\phi^{(p+[(1-\gamma)(N-B)])} - \phi^{(p)})\right],$$

where the highest number less than or equal to y is denoted by the symbol $[y]$.

4 Monte Carlo Simulations

To assess how well the suggested point (or interval) estimators perform for $\alpha, \beta, \theta, R(t)$ and $h(t)$ obtained in the proceeding sections, extensive Monte Carlo simulation experiments are carried out. From the proposed HEE distribution, when the actual value of parameters (α, β, θ) is taken as (0.8, 0.3, 0.1), we replicated 2,000 times progressively Type-II censored samples utilizing several choices of n (number of test items), m (number of effective test items) and $R_i, i = 1, \ldots, m$ (progressive mechanism). At distinct time $t = 0.1$, using the same true parameter values of α, β and θ, the respective true values of $R(t)$ and $h(t)$ are 0.762 and 2.472. For different choices of n, such as $n = 40$ (moderate) and 80 (large), different values of the failure proportion (FP) $\frac{m}{n} \times 100\%$ such as 50% and 80% are considered. Recall that, in progressive Type-II censoring plan, when the FP achieves its pre-fixed value, the test

stops. Four distinct censoring schemes are also taken into consideration in order to assess the behavior of the removal patterns $R_i,\ i = 1, \ldots, m$, namely

$$\text{S1}: \quad R_1 = n - m, \qquad R_i = 0 \quad \text{for} \quad i \neq 1,$$

$$\text{S2}: \quad R_{\frac{m}{2}} = n - m, \qquad R_i = 0 \quad \text{for} \quad i \neq m/2,$$

$$\text{S3}: \quad R_m = n - m, \qquad R_i = 0 \quad \text{for} \quad i \neq m,$$

$$\text{S4}: \quad R_1 = R_2 = \cdots = R_m = 0 \quad \text{and} \quad n = m.$$

The proposed schemes Si for $i = 1, 2, 3, 4$ behave similarly to the left progressive (when the survival $n-m$ units are removed at the time of first failure occurs), middle progressive (when the survival $n-m$ units are removed at the time of $(m/2)$th failure occurs), Type-II censoring (when the survival $n - m$ units are removed at the time of mth failure occurs), and complete sampling (when all experimental units failed), respectively. To discuss the behavior of the gamma density priors on the Bayesian analysis, two prior sets of $(a_k, b_k),\ k = 1, 2, 3$, are considered, called Prior-I: $(a_1, a_2, a_3) = (4, 1.5, 0.5)$ and $b_k = 5,\ k = 1, 2, 3$ and Prior-II: $(a_1, a_2, a_3) = (8, 3, 1)$ and $b_k = 10,\ k = 1, 2, 3$. The posterior distribution will be reduced proportionally to the likelihood function if the researcher does not have prior knowledge about the model parameters of the lifespan distribution under consideration. Using the M-H algorithm described in Section 3, we generate 12,000 MCMC samples from the conditional posterior distributions and then the first 2,000 MCMC iterations have been discarded as burn-in. The starting values of α, β and θ used to run the M-H algorithm have been chosen to be their classical estimates. To check the convergence of the generated sequences of α, β, θ, $R(t)$ and $h(t)$, both autocorrelation and trace plots of their 10,000 MCMC variates (for $n[FP\%] = 40[50\%]$ and S1 as an example) are shown in Fig. 2. It shows that the MCMC iterations for all unknown parameters are effectively mixed, so all estimated results are reasonable. However, using the lasting 10,000 MCMC iterations, the Bayes estimates (through SE and GE (for $\delta(= -2, +2)$) loss functions) as well as the 95% HPD intervals of α, β, θ, $R(t)$ and $h(t)$ are computed.

Frequentist and Bayes estimates of α, β, θ, $R(t)$ and $h(t)$ (say ϕ "for briefly") are compared using their respective root mean squared-error (RMSE) and mean absolute bias (MAB) values obtained as follows:

$$\text{RMSE}(\check{\phi}) = \sqrt{\frac{1}{\mathscr{S}} \sum_{j=1}^{\mathscr{S}} \left(\check{\phi}^{(j)} - \phi\right)^2},$$

and

$$\text{MAB}(\check{\phi}) = \frac{1}{\mathscr{S}} \sum_{j=1}^{\mathscr{S}} \left|\check{\phi}^{(j)} - \phi\right|,$$

where $\check{\phi}$ is an estimate of ϕ using any estimation method and $\mathscr{S}$ is the number of generated samples. The ACIs and HPD credible interval estimates of the unknown parameters are also compared using their average confidence lengths (ACLs) and coverage probabilities (CPs), which are provided by

$$\text{ACL}_{(1-\gamma)\%}(\phi) = \frac{1}{\mathscr{S}} \sum_{j=1}^{\mathscr{S}} \left(\mathscr{U}_{\check{\phi}^{(j)}} - \mathscr{L}_{\check{\phi}^{(j)}}\right),$$

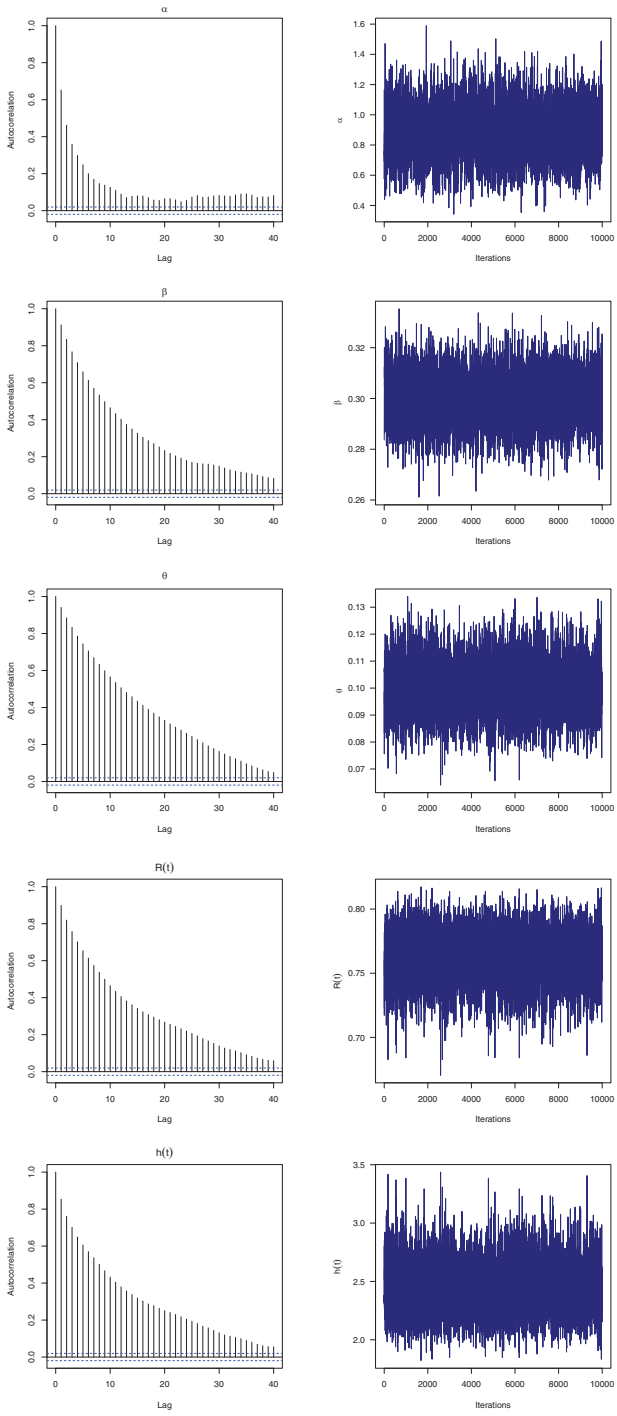

Figure 2: Autocorrelation (left) and Trace (right) plots for MCMC draws of α, β, θ, $R(t)$ and $h(t)$

and

$$\mathrm{CP}_{(1-\gamma)\%}(\phi) = \frac{1}{\mathscr{S}} \sum_{j=1}^{\mathscr{S}} \mathbf{1}_{\left(\mathscr{L}_{\check{\phi}(j)}, \mathscr{U}_{\check{\phi}(j)}\right)}(\phi),$$

where $\mathbf{1}(\cdot)$ is the indicator function and $\mathscr{L}(\cdot)$ and $\mathscr{U}(\cdot)$ denote the lower and upper bounds, respectively, of $(1-\gamma)\%$ ACIs or HPD credible interval of ϕ.

Following Henningsen et al. [14] and Plummer et al. [23], all numerical evaluations for both classical and Bayesian estimators of Ψ were conducted via 'maxLik' and 'coda' packages, respectively in R 4.1.2 software. Elshahhat et al. [24] recommended the same packages. Graphically, the corresponding simulated values (including RMSE, MAB, ACL and CP) for α, β, θ, $R(t)$ and $h(t)$ are displayed with heatmap plots, see Figs. 3–7, respectively. For specialization, based on Prior-I (say P1) as an example, several notations have been used such as (i) Bayes estimates based on SE loss are symbolized by "SE-P1" and (ii) Bayes estimates based on GE loss using $\delta = -2$ and $+2$ are symbolized by "GE1-P1" and "GE2-P1", respectively. All simulation results for the various considered tests are also provided (see Tables S1–S10) in the supplementary file.

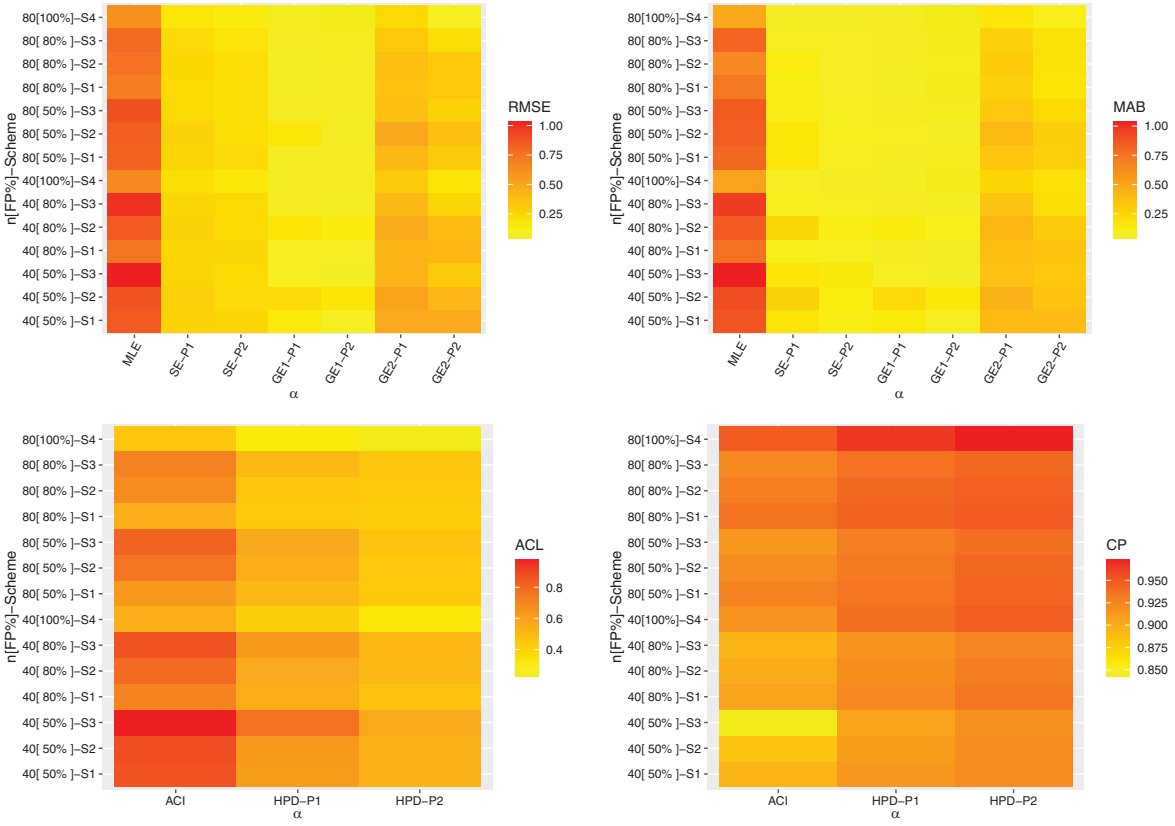

Figure 3: Heatmap plots for the estimation results of α

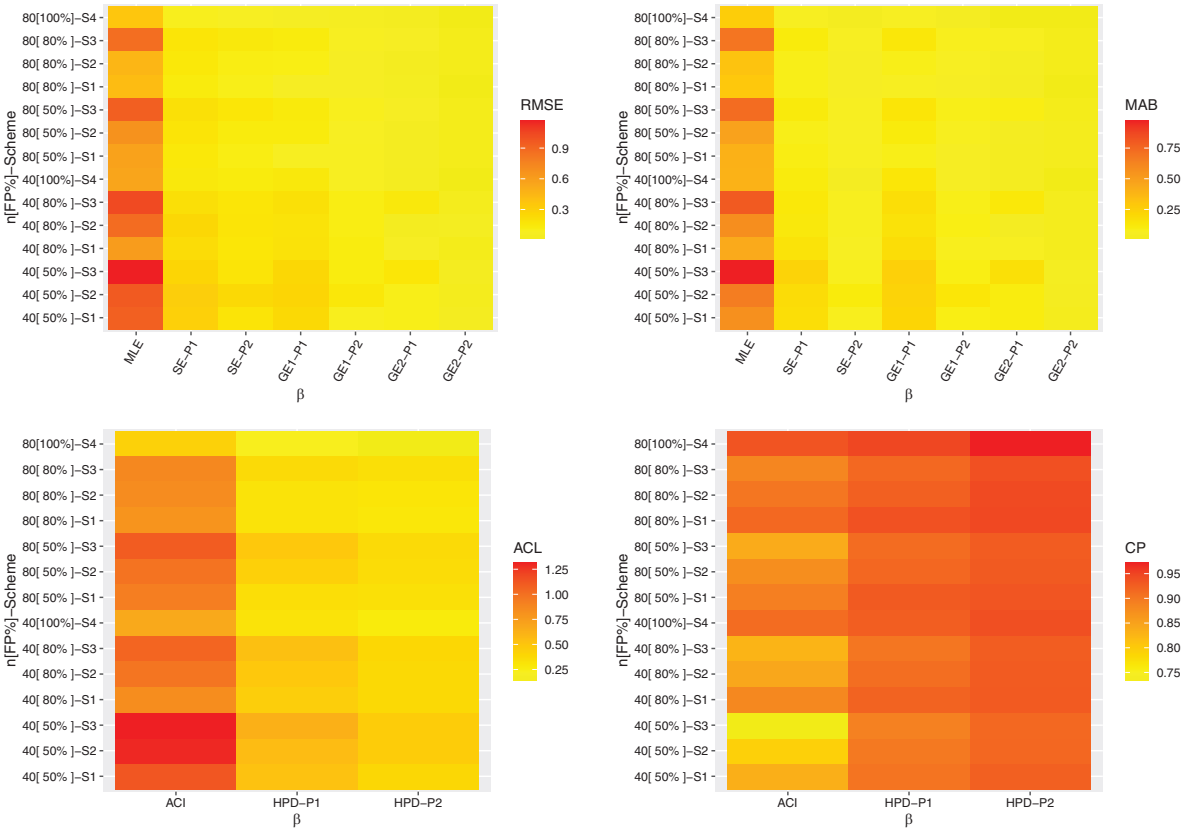

Figure 4: Heatmap plots for the estimation results of β

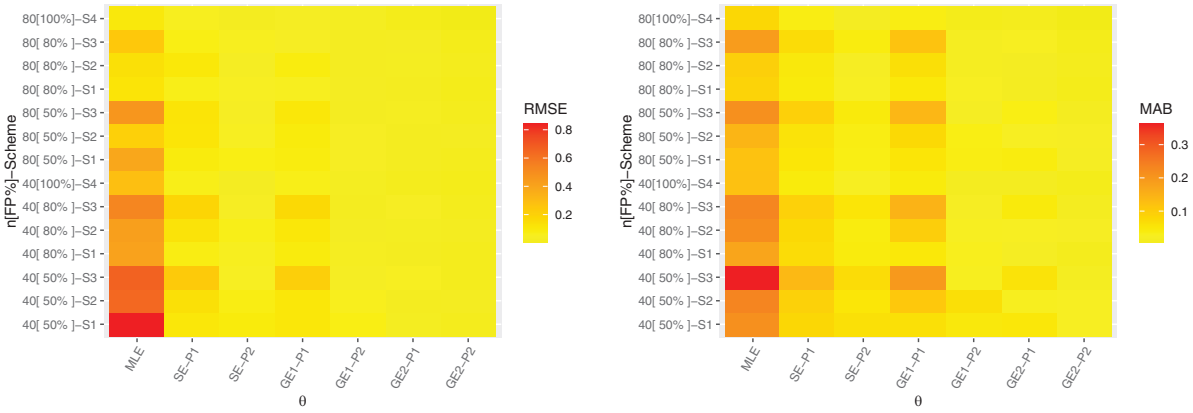

Figure 5: (Continued)

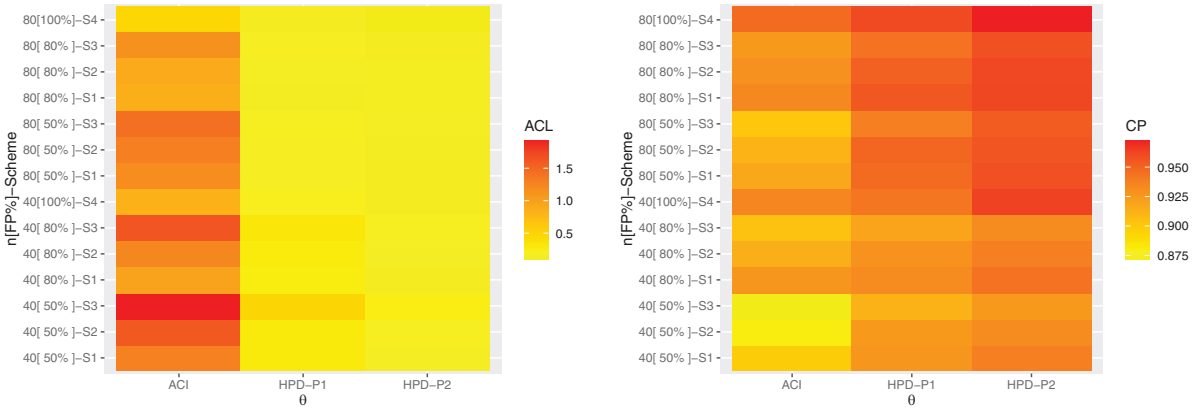

Figure 5: Heatmap plots for the estimation results of θ

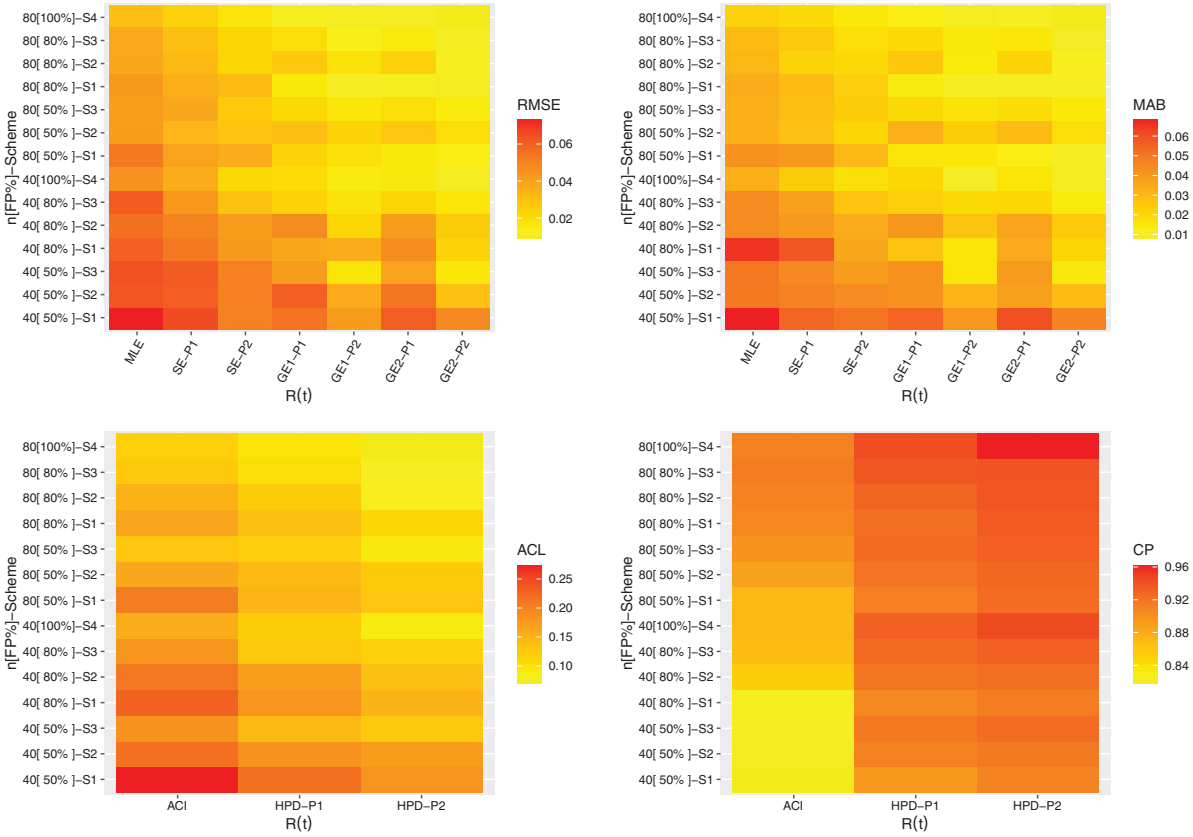

Figure 6: Heatmap plots for the estimation results of $R(t)$

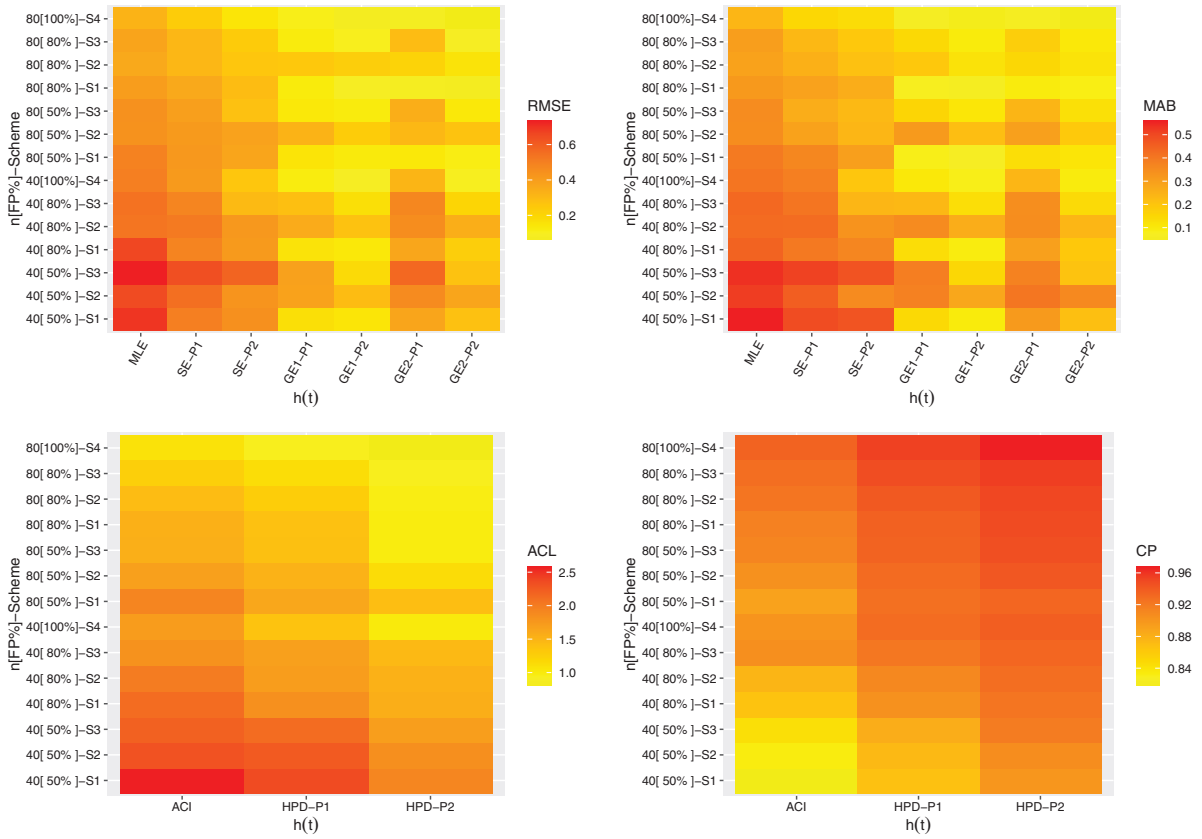

Figure 7: Heatmap plots for the estimation results of $h(t)$

From Figs. 3–7, some observations can be drawn as:

- All offered estimates of the unknown HEE parameters α, β and θ (or its reliability characteristics $R(t)$ and $h(t)$) are excellent in terms of the smallest RMSE, MAB and ACL values and highest CP values.
- All estimated estimations perform satisfactorily as n (or FP) rises. All estimates also behave in the same way when $\sum_{i=1}^{m} R_i$ goes down.
- Comparing the point estimation methods of α, β, θ, $R(t)$ and $h(t)$, due to the MCMC estimates included additional prior information, the MCMC estimates performed better against the GE loss than the SE loss and both are more favorable compared to the classical estimates in terms of the smallest RMSE and MAB values.
- Comparing the proposed interval estimation methods of α, β, θ, $R(t)$ and $h(t)$s, in terms of the smallest ACL values and highest CP values, the HPD interval estimates of all unknown parameters behave preferably than others. In addition, in most cases, the CPs are below (or close to) the nominal level.
- The Prior-II behaves better than the Prior-I in terms of the lowest values of RMSE, MAB, and ACL, as well as the greatest values of CP, when comparing the Bayes estimates of all unknown parameters based on Priors I and II. This outcome was expected because the associated variance of Prior-II is lower than that of Prior-I.

- Comparing S1 and S3, in terms of the smallest RMSE, MAB and ACL values and highest CP values, it is observed that the proposed estimates of α, β and θ based on the censoring plan S1 perform better compared to S3 while that of $R(t)$ and $h(t)$ based on S3 perform better than S1.
- Among the calculated estimates, the methods for estimating model parameters or reliability properties show superior performance using S4 which usually provides the best results for all unknown parameters as expected. It is an expected result because the acquired estimates have been obtained based on all information included in the complete sample.
- Finally, when data is acquired from a progressively Type-II censored sampling plan, the Bayes inferences based on the M-H algorithm are advised to estimate the unknown parameters and the reliability measures of the HEE lifespan distribution.

5 Optimal Progressive Censoring Plan

The topic of how to pick a specific progressive censoring scheme naturally arises. Should we select a certain plan just on the basis of convenience or should we consider some statistical factors? The statistical literature has drawn a lot of attention to the topic of selecting the best censoring schemes. Finding the progressive censoring plan that provides the most information about the unknown parameters among all potential progressive censoring plans is necessary for choosing the best sampling approach. Here, probable censoring schemes relate to all $Ri, i = 1, dots, m$ mixtures for specified n and m, where $m+\sum_{i=1}^{m} R_i = n$. References for additional information on the best censoring schemes include Ng et al. [25], Kundu [26] and Pradhan et al. [27]. Four optimality criteria that have been extensively used in the literature are taken into account in this study. Practically speaking, as we have already indicated, we must choose the filtering method that gives us the greatest details on the parameters. Table 1 outlines a few often used optimal criteria to help us select the most appropriate progressive censoring.

Table 1: Some optimal censoring plan criteria

Criterion	Method
I	Max trace $(\mathbf{I}_{3\times3}(\hat{\mathbf{\Psi}}))$
II	Min trace $(\mathbf{I}^{-1}_{3\times3}(\hat{\mathbf{\Psi}}))$
III	Min det $(\mathbf{I}^{-1}_{3\times3}(\hat{\mathbf{\Psi}}))$
IV	Min $\widehat{var}\ (\log(\hat{T}_q)), 0 < q < 1$

We wish to maximize the trace of the observed FI matrix in terms of criterion I. Additionally, we want to reduce the determinant and trace of $\mathbf{I}^{-1}_{3\times3}(\hat{\boldsymbol{\xi}})$ for criterions II and III, respectively. The variance of the logarithmic MLE of the q^{th} quantile is to be minimized according to criterion IV, denoted by $\widehat{var}(\log(\hat{T}_q))$. As a result, the logarithmic for $\hat{T}_q$ for the HEE distribution is supplied by

$$\log(\hat{T}_q) = -\frac{1}{\hat{\alpha}\hat{\beta}} \log\left[\frac{(1-q)^{\hat{\alpha}}}{\hat{\tilde{\theta}}(1-q)^{\hat{\alpha}} + \hat{\theta}}\right].$$

The variance of $\log(\hat{T}_q)$ can be approximated using the delta approach. The highest value of criterion I and the lowest values of criterions II, III, and IV are indicative of the optimal progressive censoring plan.

6 Real-Life Applications

In this section, two real-world data sets from the engineering and veterinary industries are investigated to see how the estimating approaches suggested in this study perform in actual use.

6.1 Turbocharger Data

The time-to-failure (10^3) of forty sets of turbochargers in one type of diesel engine will be used in this application from the engineering sector, see Table 2. Guerra et al. [28] reanalyzed this data set after it was provided by Xu et al. [29].

Table 2: Failure times of 40 turbochargers

1.6	2.0	2.6	3.0	3.5	3.9	4.5	4.6	4.8	5.0
5.1	5.3	5.4	5.6	5.8	6.0	6.0	6.1	6.3	6.5
6.5	6.7	7.0	7.1	7.3	7.3	7.3	7.7	7.7	7.8
7.9	8.0	8.1	8.3	8.4	8.4	8.5	8.7	8.8	9.0

We fit the HEE distribution and compare it to other seven lifetime distributions as its competitors, including the alpha power exponential (APE), generalized-exponential (GE), Nadarajah-Haghighi (NH), Weibull (W), G, Lomax (L), and exponential (E) distributions. For $x > 0$ and $\beta, \theta > 0$, the corresponding PDFs of these distributions are presented in Table 3.

Table 3: Competing statistical models of the HEE distribution

Model	$f(x)$	Author(s)
APE	$\theta(\beta-1)^{-1}\log(\beta)e^{-\theta x}\beta^{1-e^{-\theta x}}$	Mahdavi et al. [2]
GE	$\theta\beta e^{-\beta x}(1-e^{-\beta x})^{\theta-1}$	Gupta et al. [30]
NH	$\theta\beta(1+\beta x)^{\theta-1}\exp(1-(1+\beta x)^{\theta})$	Nadarajah et al. [1]
W	$\beta\theta x^{\beta-1}e^{-\theta x^{\beta}}$	Weibull [31]
G	$\frac{\theta^{\beta}}{\Gamma(\beta)}x^{\beta-1}e^{-\theta x}$	Johnson et al. [32]
L	$\beta\theta(1+\theta x)^{-(\beta+1)}$	Lomax [33]
E	$\theta e^{-\theta x}$	Johnson et al. [32]

Several model selection criteria, including negative log–likelihood (NL), Akaike's (A), Bayesian (B), consistent Akaike's (CA), and Hannan–Quinn (HQ) information criteria, are utilized to show the HEE distribution's utility in comparison to its rival models. Three alternative goodness–of–fit statistics, namely, Anderson–Darling (AD), Cramér–von Mises (CvM), and Kolmogorov–Smirnov (KS) (with its p-value) statistics are also used to assess the validity of the HEE model in comparison to other competitor models. Based on these measures, the best distribution corresponds to the lowest value of A, B, CA, HQ, AD, CvM and KS statistics as well as to the highest p-value via $\mathscr{R}$ software and 'AdequacyModel' package proposed by Marinho et al. [34], all unknown parameters are estimated using the maximum likelihood method and their standard–errors (St.Errs) are also computed and reported in Table 4. However, the estimated values of the given goodness–of–fit measures under the turbochargers data set are presented in Table 5. It is evident that the HEE distribution is the good

distribution compared to the other distributions under the turbochargers data. We further draw quantile–quantile plots of the HEE distribution and the competitive models based on the same given data, see Fig. 8. Moreover, the histogram and the fitted densities as well as the plot of fitted/empirical reliability functions of all considered distributions are displayed in Figs. 9a and 9b, respectively. Graphical presentations in Figs. 8 and 9 support the results in Table 5 which indicate that the HEE distribution is the best model to fit the turbochargers data compared to all given distributions listed in Table 3.

Table 4: Summary fit of the HEE distribution and other competing models from turbochargers data

Model	α		β		θ	
	Estimate	St.Err	Estimate	St.Err	Estimate	St.Err
HEE	0.0801	0.1294	7.9269	12.101	1063.5	1494.9
APE	–	–	2430.7	2422.7	0.4105	0.0356
GE	–	–	9.5142	2.8959	0.4498	0.0578
NH	–	–	26.932	16.541	0.0045	0.0028
W	–	–	3.8725	0.5176	6.9200	0.2947
G	–	–	7.7487	1.6832	0.8065	0.1809
L	–	–	5.3062	2.2487	29.275	12.507
E	–	–	–	–	0.1599	0.0253

Table 5: Goodness-of-fit results of the HEE distribution and other competing models from turbochargers data

Model	NL	A	B	CA	HQ	AD	CvM	KS (p-value)
HEE	80.2971	166.5941	171.6608	167.2608	168.4261	0.2630	0.0355	0.0930 (0.879)
APE	90.3055	184.6111	187.9888	184.9354	185.8323	1.3497	0.2032	0.1763 (0.166)
GE	90.1427	184.2853	187.6631	184.6097	185.5066	1.7601	0.2757	0.1541 (0.298)
NH	102.146	208.2920	211.6698	208.6163	209.5133	0.8742	0.1238	0.3652 (0.015)
W	82.4755	168.9510	172.3288	169.2754	170.1723	0.5730	0.0770	0.1077 (0.742)
G	87.4104	178.8209	182.1986	179.1452	180.0422	1.3616	0.2053	0.1281 (0.563)
L	116.7596	237.5193	240.8971	237.8437	238.7406	1.5160	0.2322	0.3817 (0.005)
E	113.3192	228.6385	230.3274	228.7438	229.2492	1.3689	0.2065	0.3630 (0.009)

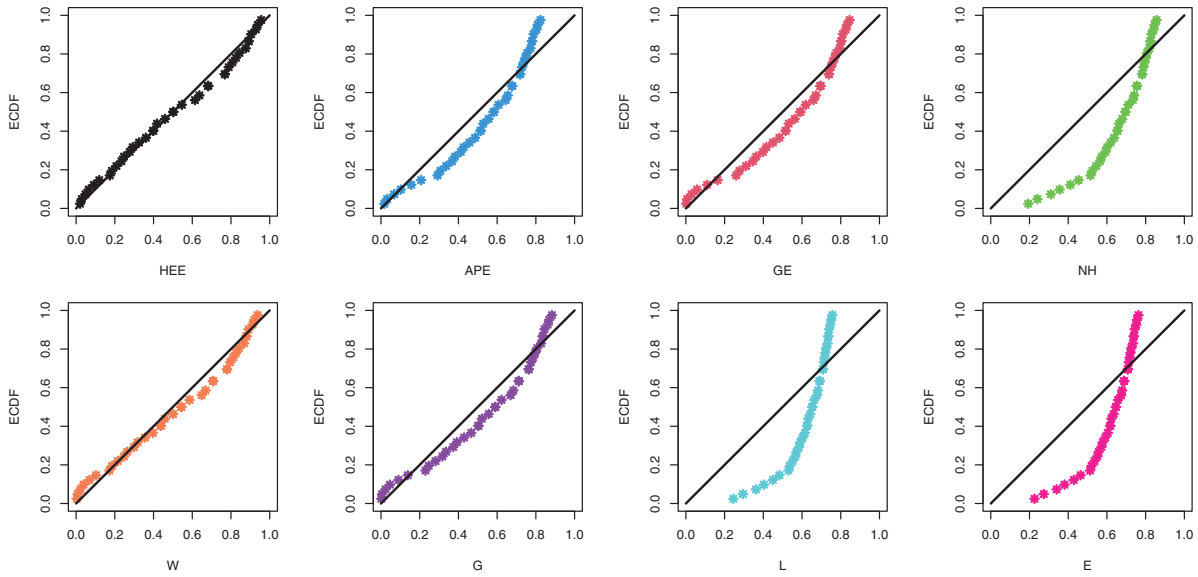

Figure 8: The quantile-quantile plots of the HEE distribution and other competing models using turbochargers data

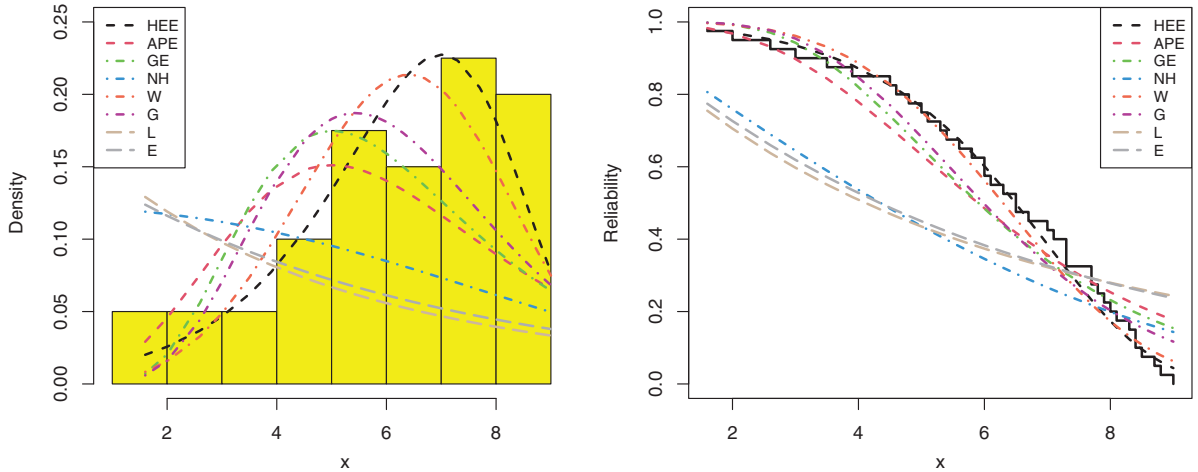

(a) PDFs (b) RFs

Figure 9: Estimated densities and reliability functions of the HEE distribution and other competing models using turbochargers data

From the complete turbochargers data, three different progressively Type-II censored samples with $m = 20$ are generated, where $\mathbf{R} = (2, 0, 0, 0, 2)$ is denoted by $\mathbf{R} = (2, 0^*3, 2)$ and reported in Table 6. Using Table 6, the maximum likelihood and Bayes estimates with their St.Errs of α, β, θ, $R(t)$ and $h(t)$ at given time $t = 5$ are calculated and provided in Table 7. Also, 95% two-sided ACI and HPD credible interval estimates with their interval lengths are obtained and presented in Table 8.

Table 6: Three progressively Type-II censored samples from turbochargers data

Sample	Scheme	Censored data									
S_1	$(10, 10, 0^*18)$	1.6	5.3	7.0	7.1	7.3	7.3	7.3	7.7	7.7	7.8
		7.9	8.0	8.1	8.3	8.4	8.4	8.5	8.7	8.8	9.0
S_2	$(0^*9, 10, 10, 0^*9)$	1.6	2.0	2.6	3.0	3.5	3.9	4.5	4.6	4.8	5.0
		6.5	8.0	8.1	8.3	8.4	8.4	8.5	8.7	8.8	9.0
S_3	$(0^*18, 10, 10)$	1.6	2.0	2.6	3.0	3.5	3.9	4.5	4.6	4.8	5.0
		5.1	5.3	5.4	5.6	5.8	6.0	6.0	6.1	6.3	7.8

Table 7: Point estimates of α, β, θ, $R(t)$ and $h(t)$ from turbochargers data

Sample	Par.	MLE		SE		GE					
$\delta \rightarrow$						-3		-0.03		3	
		Est.	St.Err	Est.	St.Err	Est.	St.Err	Est.	St.Err	Est.	St.Err
S_1	α	0.2384	0.1180	0.2378	3.47×10^{-5}	0.2381	3.91×10^{-4}	0.2377	6.93×10^{-4}	0.2374	1.00×10^{-3}
	β	3.7836	1.5999	3.7826	4.98×10^{-5}	3.7827	9.57×10^{-4}	3.7826	9.96×10^{-4}	3.7826	1.04×10^{-3}
	θ	5173.1	11.881	5173.1	5.02×10^{-5}	5173.1	8.90×10^{-4}	5173.1	8.90×10^{-4}	5173.1	8.90×10^{-4}
	$R(5)$	0.9302	0.0151	0.9305	3.43×10^{-5}	0.9306	3.76×10^{-4}	0.9305	3.00×10^{-4}	0.9304	2.23×10^{-4}
	$h(5)$	0.0654	0.0137	0.0651	4.21×10^{-5}	0.0662	8.03×10^{-4}	0.0646	8.04×10^{-4}	0.0630	2.43×10^{-3}
S_2	α	0.0723	0.0338	0.0717	2.24×10^{-5}	0.0720	3.67×10^{-4}	0.0716	7.82×10^{-4}	0.0711	1.22×10^{-3}
	β	7.6421	2.7495	7.6412	4.98×10^{-5}	7.6412	9.59×10^{-4}	7.6412	9.78×10^{-4}	7.6411	9.98×10^{-4}
	θ	1064.5	5.2321	1064.4	5.00×10^{-5}	1064.4	9.05×10^{-4}	1064.5	9.05×10^{-4}	1064.4	9.05×10^{-4}
	$R(5)$	0.8255	0.0332	0.8273	9.30×10^{-5}	0.8277	2.16×10^{-3}	0.8271	1.54×10^{-3}	0.8264	9.00×10^{-4}
	$h(5)$	0.1123	0.0229	0.1111	9.32×10^{-5}	0.1142	1.89×10^{-3}	0.1096	2.72×10^{-3}	0.1049	7.47×10^{-3}
S_3	α	4.5181	3.6838	4.4927	2.47×10^{-4}	4.4933	2.48×10^{-2}	4.4925	2.56×10^{-2}	4.4917	2.65×10^{-2}
	β	0.2151	0.1065	0.2141	4.52×10^{-5}	0.2145	5.75×10^{-4}	0.2140	1.14×10^{-3}	0.2134	1.72×10^{-3}
	θ	44.144	13.593	44.144	4.94×10^{-5}	44.143	1.11×10^{-3}	44.143	1.11×10^{-3}	44.143	1.12×10^{-3}
	$R(5)$	0.7400	0.0625	0.7445	1.25×10^{-4}	0.7454	5.35×10^{-3}	0.7441	4.10×10^{-3}	0.7428	2.82×10^{-3}
	$h(5)$	0.1612	0.0369	0.1584	7.52×10^{-5}	0.1598	1.36×10^{-3}	0.1577	3.48×10^{-3}	0.1554	5.73×10^{-3}

Table 8: Interval estimates of α, β, θ, $R(t)$ and $h(t)$ from turbochargers data

Sample	Par.	ACI			HPD		
		Lower	Upper	Length	Lower	Upper	Length
S_1	α	0.0072	0.4696	0.4624	0.2243	0.2515	0.0271
	β	0.6479	6.9193	6.2714	3.7637	3.8027	0.0391
	θ	5149.8	5196.3	46.576	5173.2	5173.1	0.0394
	$R(5)$	0.9006	0.9598	0.0592	0.9168	0.9435	0.0267
	$h(5)$	0.0387	0.0922	0.0535	0.0493	0.0820	0.0326

(Continued)

Table 8 (continued)

Sample	Par.	ACI			HPD		
		Lower	Upper	Length	Lower	Upper	Length
S_2	α	0.0060	0.1387	0.1327	0.0629	0.0804	0.0175
	β	2.2532	13.031	10.778	7.6214	7.6604	0.0389
	θ	1054.2	1074.7	20.509	1064.5	1064.5	0.0393
	$R(5)$	0.7604	0.8906	0.1302	0.7897	0.8623	0.0726
	$h(5)$	0.0675	0.1572	0.0897	0.0766	0.1490	0.0724
S_3	α	0.0000	11.738	11.738	4.3972	4.5900	0.1928
	β	0.0064	0.4238	0.4175	0.1970	0.2325	0.0355
	θ	17.502	70.787	53.285	44.124	44.162	0.0385
	$R(5)$	0.6176	0.8624	0.2448	0.6962	0.7941	0.0979
	$h(5)$	0.0888	0.2335	0.1448	0.1282	0.1872	0.0590

Since no prior information is available for HEE parameters α, β and θ from turbochargers data, non-informative priors, i.e., $a_i = b_i = 0,\ i = 1, 2, 3$, are used to carry out the Bayesian analysis from both SE and GE (for $\delta(= -3, -0.03, +3)$) loss functions. To run calculations, we have taken 1×10^{-4} for all given hyper-parameters. Using the MCMC algorithm described in Section 3, the first 10,000 iterations have been discarded from 50,000 MCMC samples in order to eliminate effects from the initial values. The initial guesses of α, β and θ were taken to be their classical estimates. It is observed, from Tables 7 and 8, that the Bayes estimates of α, β, θ, $R(t)$ and $h(t)$ perform better than the frequentist estimates in terms of their St.Errs as well as the corresponding lengths of the HPD interval estimates are narrow down compared to the ACIs. In addition, some vital properties for the MCMC outputs of all unknown parameters after burn-in, namely: mean, mode, quartiles (Q_i for $i = 1, 2, 3$), standard deviation (St.D) and skewness (Skew.) are calculated and presented in Table 9.

Table 9: Vital properties of MCMC outputs of α, β, θ, $R(t)$ and $h(t)$ from turbochargers data

Sample	Par.	Mean	Mode	Q_1	Q_2	Q_3	St.D	Skew.
S_1	α	0.23785	0.23643	0.23320	0.23792	0.24260	0.00695	−0.05050
	β	3.78264	3.78977	3.77596	3.78264	3.78931	0.00996	0.01078
	θ	5173.09	5173.08	5173.09	5173.09	5173.11	0.01004	0.00173
	$R(5)$	0.93054	0.93171	0.92607	0.93081	0.93531	0.00687	−0.24748
	$h(5)$	0.06514	0.06357	0.05925	0.06470	0.07053	0.00841	0.32828
S_2	α	0.07169	0.07128	0.06876	0.07176	0.07479	0.00448	−0.14659
	β	7.64117	7.64033	7.63450	7.64113	7.64788	0.00996	−0.01944
	θ	1064.48	1064.47	1064.47	1064.48	1064.484	0.01000	−0.01400
	$R(5)$	0.82729	0.83005	0.81488	0.82804	0.84012	0.01861	−0.17590
	$h(5)$	0.11112	0.10786	0.09807	0.10982	0.12319	0.01864	0.34268

(Continued)

Table 9 (continued)

Sample	Par.	Mean	Mode	Q_1	Q_2	Q_3	St.D	Skew.
S_3	α	4.49275	4.37610	4.45936	4.49177	4.52583	0.04947	0.06349
	β	0.21414	0.20656	0.20807	0.21414	0.22015	0.00903	0.02330
	θ	44.1436	44.1346	44.1368	44.1436	44.1502	0.00989	0.02942
	$R(5)$	0.74453	0.75410	0.72796	0.74490	0.76156	0.02498	−0.08247
	$h(5)$	0.15838	0.14053	0.14821	0.15836	0.16848	0.01505	0.00122

In MCMC iterations, the convergence of simulated chains of each unknown parameter must be checked. Therefore, based on the data set of S_1 as an example, trace plots based on 40,000 chain values of α, β, θ, $R(t)$ and $h(t)$ are plotted and displayed in Fig. 10. Furthermore, the associated histograms using the Gaussian kernel for 40,000 MCMC iterations of α, β, θ, $R(t)$ or $h(t)$ are also shown in Fig. 10. For specification, in each trace plot, the sample mean and two bounds of 95% HPD interval are expressed by soled and dashed horizontal lines, respectively, as well as in each histogram plot, the sample mean is plotted by vertical dash–dotted line. Fig. 10 shows that the proposed MCMC algorithm converges well and the size of burn–in sample is enough to eliminate the effect of the initial guesses. It also demonstrates that the generated posteriors of α, β, θ, $R(t)$ and $h(t)$ behave almost symmetrically. In the supplementary file (see Figs. S1–S2), the MCMC plots obtained from samples S_2 and S_3 of α, β, θ, $R(t)$ and $h(t)$ are presented.

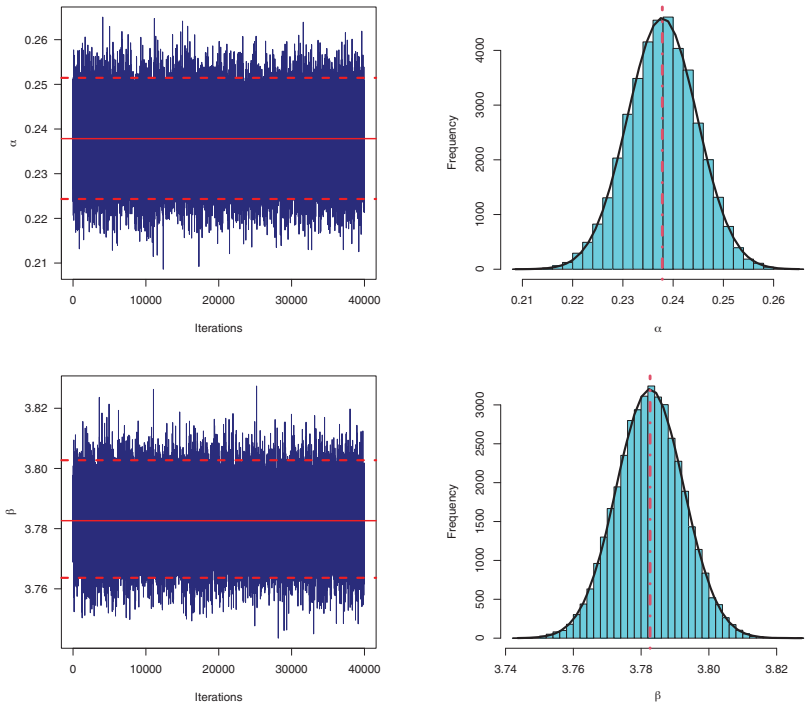

Figure 10: (Continued)

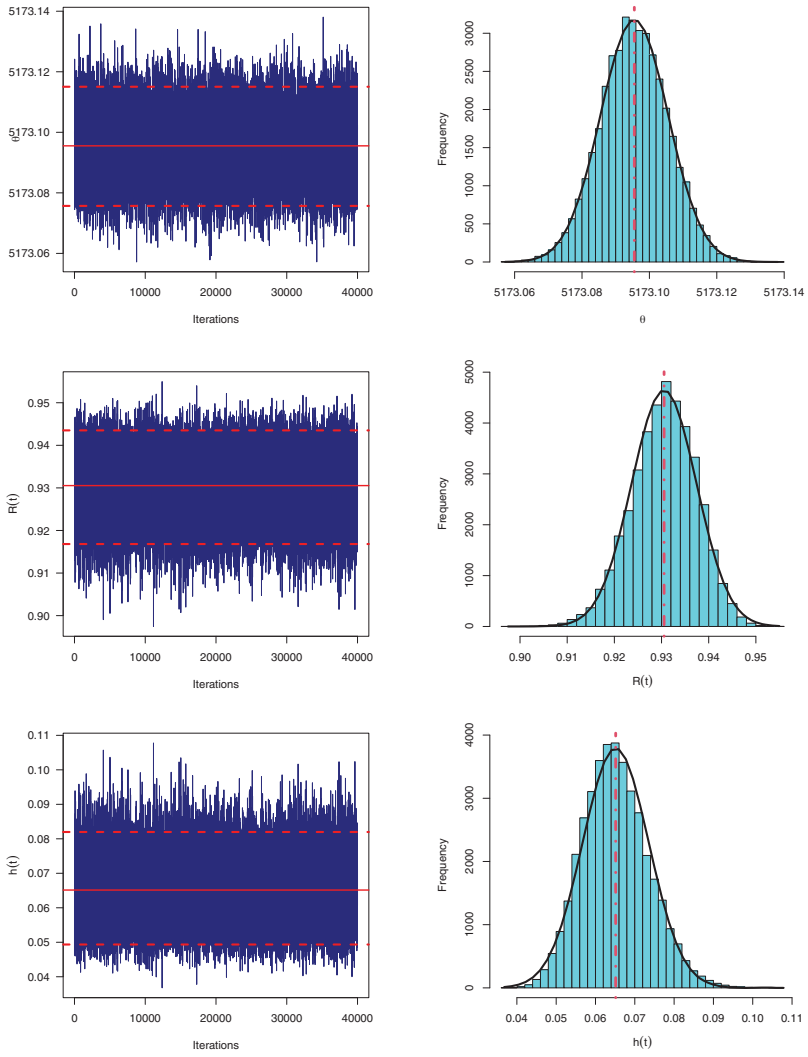

Figure 10: Trace plots (left) and Histogram plots (right) for simulated MCMC samples of α, β, θ, $R(t)$ and $h(t)$ from turbochargers data

On the basis of the data from the turbochargers, the problem of selecting the optimal censoring scheme out of all available censoring methods is also examined. The recommended optimum criteria in Table 1 are determined from the generated samples reported in Table 6 and listed in Table 10. It is clear that the progressive censoring plan $(0^*9, 10, 10, 0^*9)$ is the optimum censoring than others based on the given criterion I, II and III while $(10, 10, 0^*18)$ is the optimum censoring than others based on the criterion IV for all specified percentiles.

6.2 Guinea-Pigs Data

In this application, from veterinary medicine field, we shall provide an analysis for the survival times (in days) of 72 guinea-pigs infected with virulent tubercle bacilli. This data set was originally discussed and reported by Bjerkedal [35] and recently also explained by Chhetri et al. [36]. For

computational convenience, each lifetime point in the original guinea-pigs data set is divided by one hundred. In Table 11, the new transformed survival times are reported in ascending order.

Table 10: Optimal progressive censoring schemes from turbochargers data

Sample	1	2	3	4			
$p \rightarrow$				0.2	0.4	0.6	0.8
S_1	11145.81	143.7514	0.032497	0.0559152	0.0631377	0.073538	0.087202
S_2	40554.46	34.93527	0.004375	0.1260493	0.1345998	0.169284	0.227501
S_3	2276.636	198.3635	198.3635	0.2451898	0.3637591	1.242139	6.479739

Table 11: New transformed survival times of 72 guinea-pigs

0.10	0.33	0.44	0.56	0.59	0.72	0.74	0.77	0.92	0.93	0.96	1.00
1.00	1.02	1.05	1.07	1.07	1.08	1.08	1.08	1.09	1.12	1.13	1.15
1.16	1.20	1.21	1.22	1.22	1.24	1.30	1.34	1.36	1.39	1.44	1.46
1.53	1.59	1.60	1.63	1.63	1.68	1.71	1.72	1.76	1.83	1.95	1.96
1.97	2.02	2.13	2.15	2.16	2.22	2.30	2.31	2.40	2.45	2.51	2.53
2.54	2.54	2.78	2.93	3.27	3.42	3.47	3.61	4.02	4.32	4.58	5.55

Again, to illustrate how the HEE distribution can be used effectively to provide a better fit than the other distributions, the guinea-pigs data set is also analyzed for this purpose. From Table 11, the MLEs (with their St.Errs) of all considered distributions (given in Table 3) are calculated and reported in Table 12. Furthermore, the different goodness-of-fit criteria are also computed and reported in Table 13. It is clear, from Table 13, that the HEE distribution is the best statistical model compared to other fitted models for fitting guinea-pigs data set because it has the lowest values of the different goodness-of-fit measures and the highest p-value. Fig. 11 shows the quantile-quantile plots for the considered distributions. Furthermore, the histogram and the different fitted densities as well as the empirical and fitted reliability functions are displayed in Figs. 12a and 12b, respectively. Figs. 11 and 12 support the same findings reported in Table 13. Now, from the complete guinea-pigs data, different progressively Type-II censored samples with fixed $m = 32$ and various choices of R_i, $i = 1, \ldots, m$ are generated and listed in Table 14. The MLEs and the Bayes estimates (with their St.Errs) as well as the 95% ACI/HPD interval estimates (with their lengths) of α, β, θ, $R(t)$ and $h(t)$ (at time $t = 1$) are calculated and reported in Tables 15 and 16, respectively. Using the proposed SE and GE (for $\delta(= -3, -0.03, +3)$) loss functions, because prior knowledge about the HEE parameters from the guinea-pigs data is not available, the Bayes point estimates are obtained based on improper gamma densities when $a_i = b_i = 0$, $i = 1, 2, 3$. We also take 0.0001 for all given hyper-parameters. By running the MCMC sampler 50,000 times and omitting the first 10,000 iterations as burn-in, the Bayes point (or interval) calculations are performed. However, Table 15 shows that the point estimates of all unknown parameters obtained by frequentist and Bayesian estimation methods are almost close to each other as expected. A similar finding is also reached in the case of interval estimation.

Table 12: Summary fit of the HEE distribution and other competing models from guinea-pigs data

Model	α		β		θ	
	Estimate	St.Err	Estimate	St.Err	Estimate	St.Err
HEE	4.3287	1.5182	1.0311	0.1555	47.969	40.283
APE	–	–	21.458	9.6672	1.0522	0.0998
GE	–	–	3.6288	0.7211	1.1271	0.1316
NH	–	–	6.4260	2.6985	0.0602	0.0276
W	–	–	1.8254	0.1587	1.9960	0.1363
G	–	–	3.0981	0.4910	0.5707	0.0982
L	–	–	11.701	5.7754	20.205	10.535
E	–	–	–	–	0.5654	0.0666

Table 13: Goodness-of-fit results of the HEE distribution and other competing models from guinea-pigs data

Model	NL	A	B	CA	HQ	AD	CvM	KS (p-value)
HEE	91.8032	189.6064	196.4364	189.9593	192.3254	0.2788	0.0470	0.0713 (0.857)
APE	97.1522	198.3045	202.8578	198.4784	200.1171	0.6586	0.1134	0.1673 (0.055)
GE	94.2360	192.4721	197.0254	192.6460	194.2848	0.5224	0.0808	0.0930 (0.561)
NH	103.869	211.7381	216.2914	211.9120	213.5508	1.2021	0.2044	0.2281 (0.051)
W	95.7898	195.5796	200.1329	195.7535	197.3923	0.9711	0.1649	0.1047 (0.408)
G	94.2295	192.4591	197.0124	192.6330	194.2718	0.5985	0.0971	0.0898 (0.606)
L	115.085	234.1718	238.7251	234.3457	235.9845	0.5507	0.0873	0.2949 (0.025)
E	113.037	228.0741	230.3508	228.1312	228.9804	0.5978	0.0968	0.2944 (0.018)

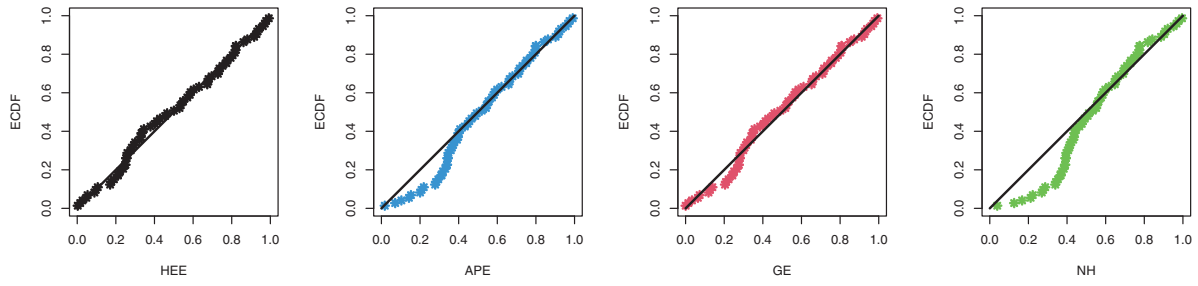

Figure 11: (Continued)

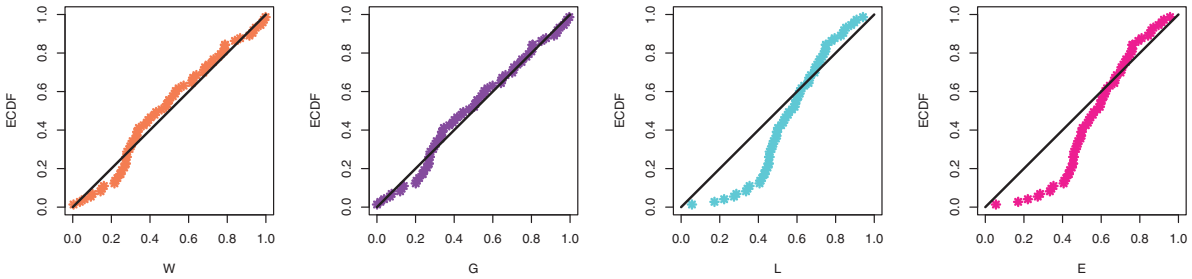

Figure 11: The quantile-quantile plots of the HEE distribution and other competing models using guinea-pigs data

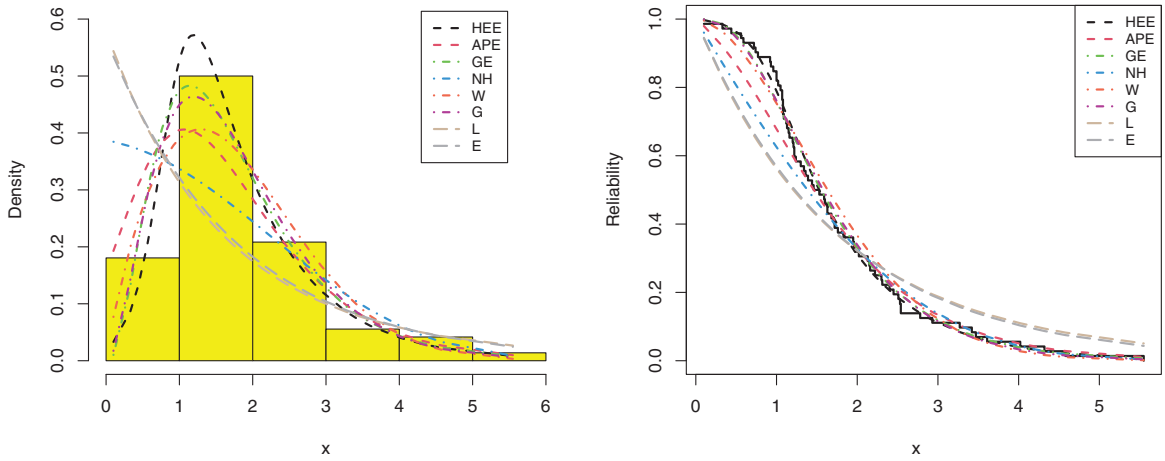

(a) PDF (b) RF

Figure 12: Estimated densities and reliability functions of the HEE distribution and other competing models using guinea-pigs data

Table 14: Three progressively Type-II censored samples from guinea-pigs data

Sample	Scheme	Censored data										
S_1	(20, 20, 0*30)	0.10	1.12	1.71	1.72	1.76	1.83	1.95	1.96	1.97	2.02	2.13
		2.15	2.16	2.22	2.30	2.31	2.40	2.45	2.51	2.53	2.54	2.54
		2.78	2.93	3.27	3.42	3.47	3.61	4.02	4.32	4.58	5.55	
S_2	(0*15, 20, 20, 0*15)	0.10	0.33	0.44	0.56	0.59	0.72	0.74	0.77	0.92	0.93	0.96
		1.00	1.00	1.02	1.05	1.07	1.53	2.45	2.51	2.53	2.54	2.54
		2.78	2.93	3.27	3.42	3.47	3.61	4.02	4.32	4.58	5.55	
S_3	(0*30, 20, 20)	0.10	0.33	0.44	0.56	0.59	0.72	0.74	0.77	0.92	0.93	0.96
		1.00	1.00	1.02	1.05	1.07	1.07	1.08	1.08	1.08	1.09	1.12
		1.13	1.15	1.16	1.20	1.21	1.22	1.22	1.24	1.30	2.15	

Table 15: Point estimates of α, β, θ, $R(t)$ and $h(t)$ from guinea-pigs data

Sample	Par.	MLE		SE		GE					
$\delta \rightarrow$						-3		-0.03		3	
		Est.	St.Err	Est.	St.Err	Est.	St.Err	Est.	St.Err	Est.	St.Err
S_1	α	2.6962	0.8659	2.6228	4.71×10^{-4}	2.6262	7.01×10^{-2}	2.6211	7.51×10^{-2}	2.6160	8.02×10^{-2}
	β	1.1954	0.2875	1.1792	2.98×10^{-4}	1.1822	1.32×10^{-2}	1.1778	1.77×10^{-2}	1.1732	2.22×10^{-2}
	θ	496.09	11.905	495.98	4.83×10^{-4}	495.98	9.95×10^{-2}	495.98	9.95×10^{-2}	495.98	9.95×10^{-2}
	$R(1)$	0.9826	0.0033	0.9841	1.21×10^{-5}	0.9841	1.59×10^{-3}	0.9841	1.58×10^{-3}	0.9841	1.57×10^{-3}
	$h(1)$	0.0577	0.0138	0.0510	4.97×10^{-5}	0.0530	4.74×10^{-3}	0.0501	7.59×10^{-3}	0.0474	1.03×10^{-2}
S_2	α	0.1004	0.0475	0.0999	4.20×10^{-5}	0.1006	2.24×10^{-4}	0.0996	8.25×10^{-4}	0.0985	1.93×10^{-3}
	β	6.1208	1.7324	6.0258	4.78×10^{-4}	6.0273	9.34×10^{-2}	6.0251	9.57×10^{-2}	6.0228	9.79×10^{-2}
	θ	54.119	11.765	54.022	4.95×10^{-4}	54.022	9.67×10^{-2}	54.022	9.70×10^{-2}	54.021	9.72×10^{-2}
	$R(1)$	0.8564	0.0320	0.8591	2.12×10^{-5}	0.8591	2.67×10^{-3}	0.8591	2.64×10^{-3}	0.8590	2.61×10^{-3}
	$h(1)$	0.2059	0.0416	0.2008	5.29×10^{-5}	0.2014	4.47×10^{-3}	0.2006	5.30×10^{-3}	0.1997	6.14×10^{-3}
S_3	α	9.9173	3.4497	9.8059	5.28×10^{-4}	9.8070	1.10×10^{-1}	9.8053	1.12×10^{-1}	9.8036	1.14×10^{-1}
	β	0.5541	0.1178	0.5366	2.23×10^{-4}	0.5403	1.39×10^{-2}	0.5348	1.94×10^{-2}	0.5293	2.49×10^{-2}
	θ	30.946	7.3592	30.853	4.71×10^{-4}	30.853	9.24×10^{-2}	30.853	9.29×10^{-2}	30.852	9.33×10^{-2}
	$R(1)$	0.8027	0.0379	0.8172	1.56×10^{-4}	0.8184	1.56×10^{-2}	0.8166	1.39×10^{-2}	0.8147	1.20×10^{-2}
	$h(1)$	0.4935	0.0872	0.4626	3.25×10^{-4}	0.4716	2.19×10^{-2}	0.4581	3.54×10^{-2}	0.4433	5.02×10^{-2}

Table 16: Interval estimates of α, β, θ, $R(t)$ and $h(t)$ from guinea-pigs data

Sample	Par.	ACI			HPD		
		Lower	Upper	Length	Lower	Upper	Length
S_1	α	0.9990	4.3934	3.3944	2.4280	2.7940	0.3660
	β	0.6320	1.7589	1.1268	1.0606	1.2938	0.2333
	θ	472.75	519.42	46.667	495.81	496.17	0.3675
	$R(1)$	0.9760	0.9891	0.0131	0.9792	0.9885	0.0093
	$h(1)$	0.0307	0.0847	0.0540	0.0332	0.0711	0.0379
S_2	α	0.0073	0.1935	0.1861	0.0835	0.1165	0.0330
	β	2.7252	9.5163	6.7910	5.8439	6.2148	0.3709
	θ	31.058	77.179	46.121	53.807	54.201	0.3940
	$R(1)$	0.7937	0.9191	0.1254	0.8505	0.8666	0.0161
	$h(1)$	0.1244	0.2873	0.1629	0.1820	0.2221	0.0401
S_3	α	3.1561	16.678	13.523	9.6018	10.016	0.4143
	β	0.3233	0.7850	0.4618	0.4528	0.6275	0.1746
	θ	16.522	45.371	28.848	30.6839	31.042	0.3584
	$R(1)$	0.7284	0.8771	0.1487	0.7546	0.8766	0.1220
	$h(1)$	0.3226	0.6644	0.3418	0.3431	0.5981	0.2550

Using the generated sample S_1 (as an example) from the guinea-pigs data, both trace and histogram plots for 40,000 MCMC simulated variates of the unknown parameters α, β, θ, $R(t)$ and $h(t)$ are displayed in Fig. 13. It indicates that the MCMC samples generated from all unknown

parameters are converged adequately. It is also evident, from the estimated Gaussian kernel, that all the generated posterior samples of the HEE parameters α, β and θ are fairly symmetrical while the generated posteriors of the survival characteristics $R(t)$ and $h(t)$ are negative and positive quite skewed, respectively. Furthermore, some vital statistics of MCMC outputs of α, β, θ, $R(t)$ and $h(t)$ such as: mean, mode, 1st quartile (Q_1), 3rd quartile (Q_3), St.D and Skew. are computed and presented in Table 17. It shows that the calculated tendency measures support the same application results in Fig. 13. From guinea-pigs data, in the supplementary file (see Figs. S3–S4), the MCMC plots obtained from samples S2 and S3 of α, β, θ, $R(t)$ and $h(t)$ are provided. Moreover, using the specific censoring schemes listed in Table 14, the calculated values of the proposed optimality criteria are provided in Table 18. It shows that the progressive censoring schemes $(20, 20, 0^*30)$ are the best compared to the other censoring schemes based on criterions IV and II, respectively; and the censoring scheme $(0^*30, 20, 20)$ is the best compared to the others based on the criterions I and III.

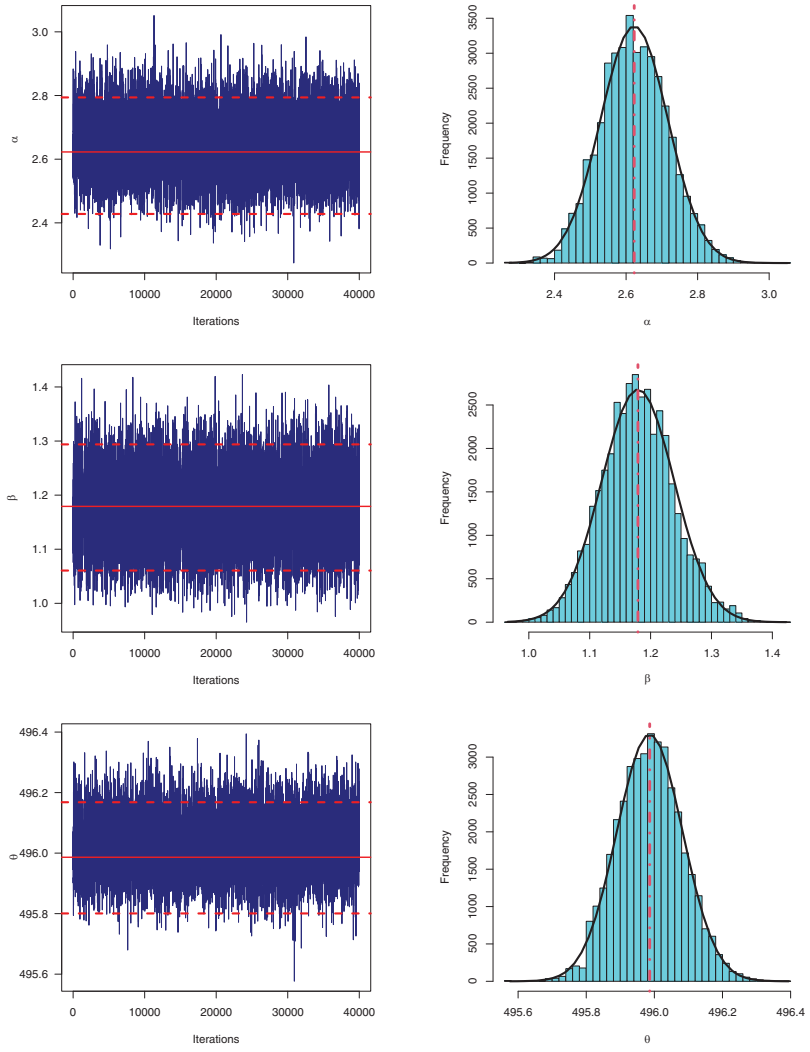

Figure 13: (Continued)

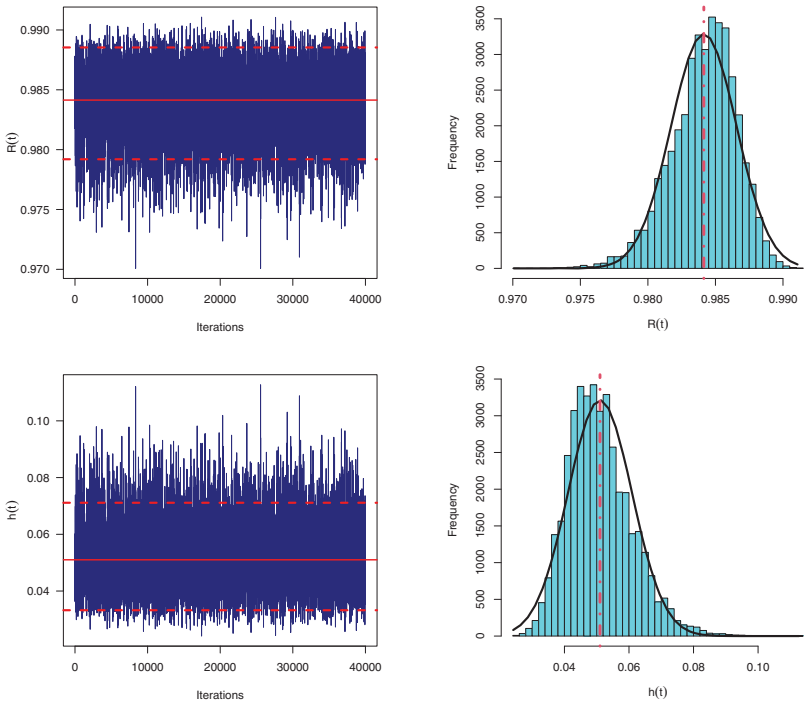

Figure 13: Trace plots (top panel) and Histogram plots (bottom panel) for simulated MCMC samples of α, β, θ, $R(t)$ and $h(t)$ from guinea-pigs data

Table 17: Vital properties of MCMC outputs of α, β, θ, $R(t)$ and $h(t)$ from guinea-pigs data

Sample	Par.	Mean	Mode	Q_1	Q_2	Q_3	St.D	Skew.
S_1	α	2.62277	2.56417	2.55656	2.62014	2.68691	0.09420	0.07891
	β	1.17921	1.18621	1.13953	1.17771	1.21759	0.05957	0.10702
	θ	495.986	495.851	495.919	495.986	496.051	0.09657	0.08720
	$R(1)$	0.98414	0.98474	0.98267	0.98437	0.98585	0.00243	−0.55429
	$h(1)$	0.05102	0.04816	0.04392	0.04989	0.05693	0.00994	0.66725
S_2	α	0.09992	0.09570	0.09443	0.09969	0.10559	0.00841	0.03833
	β	6.02583	5.89454	5.95915	6.02504	6.09046	0.09555	0.07992
	θ	54.0221	53.7727	53.9559	54.0235	54.0877	0.09895	−0.01609
	$R(1)$	0.85907	0.86395	0.85615	0.85919	0.86204	0.00423	−0.14105
	$h(1)$	0.20083	0.19002	0.19332	0.20045	0.20808	0.01058	0.19451
S_3	α	9.80589	9.66772	9.73301	9.80580	9.87597	0.10561	0.05471
	β	0.53657	0.50389	0.50416	0.53608	0.56493	0.04452	0.26831
	θ	30.8535	30.7377	30.7873	30.8528	30.9171	0.09429	0.12605
	$R(1)$	0.81718	0.84299	0.79793	0.81781	0.83990	0.03127	−0.31411
	$h(1)$	0.46258	0.41038	0.41654	0.46414	0.50459	0.06506	0.08464

Table 18: Optimal progressive censoring schemes from guinea-pigs data

Sample	1	2	3	4			
$p \rightarrow$				0.2	0.4	0.6	0.8
S_1	231.8927	142.5657	0.506579	0.012706	0.017403	0.024972	0.024972
S_2	5063.384	141.4352	0.074908	0.041076	0.051283	0.061935	0.098695
S_3	364.6434	66.07286	1.728637	0.009269	0.026071	0.088810	0.308492

7 Concluding Remarks

In this work, we have acquired both classical and Bayesian estimations of the Harris extended-exponential distribution in the existence of progressively Type-II censoring samples. The maximum likelihood approach is taken into account in the context of classical estimation in order to get the point and interval estimations of the unknown parameters, reliability, and hazard rate functions. On the other hand, under the premise of independent gamma priors, the Bayesian estimation is created based on both squared and general entropy loss functions. Due to the problematic presentation of the posterior distribution, the Markov Chain Monte Carlo technique is employed to get the Bayes estimates as well as the highest posterior density credible intervals. Monte Carlo simulations are implemented to compare the performance of the diverse point and interval estimators while accounting for various sample sizes and censoring procedures. Some optimality criteria are investigated to discover the best progressive censoring scheme. We examined two data sets for guinea pigs and turbochargers to show how the suggested estimators perform in practical environments. These applications showed also that the Harris extended-exponential distribution provides a better fit than other seven distributions in the literature. To be more specific, the numerical investigations showed that the Bayesian MCMC technique yields more accurate estimates compared to others and is recommended when the progressively Type-II censored Harris extended-exponential data exist. In future work, it may be preferable to reuse the proposed estimation methods to include competing risks or accelerated tests data.

Acknowledgement: The authors would desire to express their gratitude to the editor and the anonymous referees for useful advice and helpful comments. The authors would also like to express their full thanks to Princess Nourah bint Abdulrahman University, Riyadh, Saudi Arabia, for supporting this study.

Funding Statement: This research was funded by Princess Nourah bint Abdulrahman University Researchers Supporting Project Number (PNURSP2023R175), Princess Nourah bint Abdulrahman University, Riyadh, Saudi Arabia.

Conflicts of Interest: The authors declare that they have no conflicts of interest to report regarding the present study.

References

1. Nadarajah, S., Haghighi, F. (2011). An extension of the exponential distribution. *Statistics, 45(6),* 543–558.
2. Mahdavi, A., Kundu, D. (2017). A new method for generating distributions with an application to exponential distribution. *Communications in Statistics-Theory and Methods, 46(13),* 6543–6557.
3. Pinho, L. G. B., Cordeiro, G. M., Nobre, J. S. (2015). The Harris extended exponential distribution. *Communications in Statistics-Theory and Methods, 44(16),* 3486–3502.
4. Marshall, A. W., Olkin, I. (1997). A new method for adding a parameter to a family of distributions with application to the exponential and Weibull families. *Biometrika, 84(3),* 641–652.
5. Sultan, K. S., Alsadat, N. H., Kundu, D. (2014). Bayesian and maximum likelihood estimations of the inverse Weibull parameters under progressive Type-II censoring. *Journal of Statistical Computation and Simulation, 84(10),* 2248–2265.
6. Dey, S., Nassar, M., Maurya, R. K., Tripathi, Y. M. (2018). Estimation and prediction of Marshall–Olkin extended exponential distribution under progressively Type-II censored data. *Journal of Statistical Computation and Simulation, 88(12),* 2287–2308.
7. Kotb, M. S., Raqab, M. Z. (2019). Statistical inference for modified Weibull distribution based on progressively type-II censored data. *Mathematics and Computers in Simulation, 162(6),* 233–248.
8. Bdair, O. M., Awwad, R. R., Abufoudeh, G. K., Naser, M. F. M. (2020). Estimation and prediction for flexible Weibull distribution based on progressive type II censored data. *Communications in Mathematics and Statistics, 8(3),* 255–277.
9. Wu, M., Gui, W. (2021). Estimation and prediction for nadarajah-haghighi distribution under progressive Type-II censoring. *Symmetry, 13(6),* 999.
10. Alotaibi, R., Nassar, M., Rezk, H., Elshahhat, A. (2022). Inferences and engineering applications of alpha power weibull distribution using progressive Type-II censoring. *Mathematics, 10(16),* 2901. https://doi.org/10.3390/math10162901
11. Elshahhat, A., Rastogi, M. K. (2022). Bayesian life analysis of generalized chen's population under progressive censoring. *Pakistan Journal of Statistics and Operation Research, 18(3),* 675–702.
12. Dey, S., Elshahhat, A. (2022). Analysis of Wilson–Hilferty distribution under progressive Type-II censoring. *Quality and Reliability Engineering International, 38(7),* 3771–3796.
13. Balakrishnan, N., Cramer, E. (2014). *The art of progressive censoring*. Birkhäuser, New York: Springer.
14. Henningsen, A., Toomet, O. (2011). maxLik: A package for maximum likelihood estimation in R. *Computational Statistics, 26(3),* 443–458.
15. Panahi, H. (2017). Estimation of the Burr type III distribution with application in unified hybrid censored sample of fracture toughness. *Journal of Applied Statistics, 44(14),* 2575–2592.
16. Panahi, H. (2017). Estimation methods for the generalized inverted exponential distribution under type ii progressively hybrid censoring with application to spreading of micro-drops data. *Communications in Mathematics and Statistics, 5(2),* 159–174.
17. Greene, W. H. (2000). *Econometric analysis*, 4th edition. New York, NY, USA: Prentice-Hall.
18. Meeker, W. Q., Escobar, L. A. (2014). *Statistical methods for reliability data*. NY, USA: John Wiley & Sons.
19. Elshahhat, A., Muse, A. H., Egeh, O. M., Elemary, B. R. (2022). Estimation for parameters of life of the Marshall-Olkin generalized-exponential distribution using progressive Type-II censored data. *Complexity, 2022,* 36, 8155929. https://doi.org/ 10.1155/2022/8155929
20. Dey, S., Elshahhat, A., Nassar, M. (2022). Analysis of progressive type-II censored gamma distribution. *Computational Statistics, 38,* 481–508. https://doi.org/10.1007/s00180-022-01239-y
21. Nassar, M., Alotaibi, R., Okasha, H., Wang, L. (2022). Bayesian estimation using expected LINEX loss function: A novel approach with applications. *Mathematics, 10(3),* 436.
22. Calabria, R., Pulcini, G. (1994). An engineering approach to Bayes estimation for the Weibull distribution. *Microelectronics Reliability, 34(5),* 789–802.

23. Plummer, M., Best, N., Cowles, K., Vines, K. (2006). CODA: Convergence diagnosis and output analysis for MCMC. *R News, 6(1),* 7–11.
24. Elshahhat, A., Rastogi, M. K. (2021). Estimation of parameters of life for an inverted Nadarajah–Haghighi distribution from Type–II progressively censored samples. *Journal of the Indian Society for Probability and Statistics, 22(1),* 113–154.
25. Ng, H. K. T., Chan, C. S., Balakrishnan, N. (2004). Optimal progressive censoring plans for the Weibull distribution. *Technometrics, 46(4),* 470–481.
26. Kundu, D. (2008). Bayesian inference and life testing plan for the Weibull distribution in presence of progressive censoring. *Technometrics, 50(2),* 144–154.
27. Pradhan, B., Kundu, D. (2009). On progressively censored generalized exponential distribution. *Test, 18,* 497–515.
28. Guerra, R. R., Peña-Ramírez, F. A., Cordeiro, G. M. (2021). The Weibull Burr XII distribution in lifetime and income analysis. *Anais da Academia Brasileira de Ciências, 93(3),* 1–28.
29. Xu, K., Xie, M., Tang, L. C., Ho, S. L. (2003). Application of neural networks in forecasting engine systems reliability. *Applied Soft Computing, 2(4),* 255–268.
30. Gupta, R. D., Kundu, D. (2001). Generalized exponential distribution: Different method of estimations. *Journal of Statistical Computation and Simulation, 69(4),* 315–337.
31. Weibull, W. (1951). A statistical distribution function of wide applicability. *Journal of Applied Mechanics, 18,* 293–297.
32. Johnson, N., Kotz, S., Balakrishnan, N. (1994). *Continuous univariate distributions*, 2nd edition. NY, USA: John Wiley and Sons.
33. Lomax, K. S. (1954). Business failures: Another example of the analysis of failure data. *Journal of the American Statistical Association, 49,* 847–852.
34. Marinho, P. R. D., Silva, R. B., Bourguignon, M., Cordeiro, G. M., Nadarajah, S. (2019). AdequacyModel: An R package for probability distributions and general purpose optimization. *PLoS One, 14,* e0221487.
35. Bjerkedal, T. (1960). Acquisition of resistance in guinea pies infected with different doses of virulent tubercle bacilli. *American Journal of Hygiene, 72(1),* 130–148.
36. Chhetri, S., Mdziniso, N., Ball, C. (2022). Extended Lindley distribution with applications. *Revista Colombiana de Estadística, 45(1),* 65–83.

Supplementary Materials

Table S1: The average estimates (1st column), RMSEs (2nd column) and MABs (3rd column) of α

Table S2: The average estimates (1st column), RMSEs (2nd column) and MABs (3rd column) of β

Table S3: The average estimates (1st column), RMSEs (2nd column) and MABs (3rd column) of θ

Table S4: The average estimates (1st column), RMSEs (2nd column) and MABs (3rd column) of $R(t)$

Table S5: The average estimates (1st column), RMSEs (2nd column) and MABs (3rd column) of $h(t)$

Table S6: The ACLs (1st column) and CPs (2nd column) of 95% ACI/HPD credible intervals of α

Table S7: The ACLs (1st column) and CPs (2nd column) of 95% ACI/HPD credible intervals of β

Table S8: The ACLs (1st column) and CPs (2nd column) of 95% ACI/HPD credible intervals of θ

Table S9: The ACLs (1st column) and CPs (2nd column) of 95% ACI/HPD credible intervals of $R(t)$

Table S10: The ACLs (1st column) and CPs (2nd column) of 95% ACI/HPD credible intervals of $h(t)$

Figure S1: Trace plots (left) and Histogram plots (right) for simulated MCMC samples of α, β, θ, $R(t)$ and $h(t)$ using sample S2 from turbochargers data

Figure S2: Trace plots (left) and Histogram plots (right) for simulated MCMC samples of α, β, θ, $R(t)$ and $h(t)$ using sample S3 from turbochargers data

Figure S3: Trace plots (top panel) and Histogram plots (bottom panel) for simulated MCMC samples of α, β, θ, $R(t)$ and $h(t)$ using sample S2 from guinea-pigs data

Figure S4: Trace plots (top panel) and Histogram plots (bottom panel) for simulated MCMC samples of α, β, θ, $R(t)$ and $h(t)$ using sample S3 from guinea-pigs data